Design, synthesis and biological evaluation of novel histone deacetylase (HDAC) inhibitors derived from β-elemene scaffold

Yuan Gao, Jilong Duan, Xiawen Dang, Yinghui Yuan, Yu Wang, Xingrui He, Renren Bai, Xiang-Yang Ye & Tian Xie

Taylor & Francis
Taylor & Francis Group

RESEARCH PAPER

🔓 OPEN ACCESS | Check for updates

Design, synthesis and biological evaluation of novel histone deacetylase (HDAC) inhibitors derived from *β*-elemene scaffold

Yuan Gao[a,b], Jilong Duan[b], Xiawen Dang[b], Yinghui Yuan[b], Yu Wang[c], Xingrui He[b], Renren Bai[b], Xiang-Yang Ye[b] and Tian Xie[a,b]

[a]Institute of Traditional Chinese Medicine, Shanghai University of Traditional Chinese Medicine, Shanghai, China; [b]Key Laboratory of Elemene Class Anti-Cancer Chinese Medicines; Engineering Laboratory of Development and Application of Traditional Chinese Medicines, Collaborative Innovation Center of Traditional Chinese Medicines of Zhejiang Province, Hangzhou Normal University, Hangzhou, China; [c]Research and Development, Dalian HolleyKingkong Pharmaceutical Co. Ltd, Liaoning, China

ABSTRACT

β-Elemene is the major active ingredient of TCM anticancer drug elemene extracts. To further improve its antitumor activity and poor solubility, a polar HDACi pharmacophore was incorporated its scaffold. Systematic SAR studies led to the discovery of compounds **27f** and **39f**, which exhibited potent inhibitory activity against HDACs (HDAC1: IC_{50} = 22 and 9 nM; HDAC6: 8 and 14 nM, respectively). In cellular levels, **27f** and **39f** significantly inhibited cell proliferation of five tumour cell lines (IC_{50}: 0.79 - 4.42 µM). Preliminary mechanistic studies indicated that **27f** and **39f** efficiently induced cell apoptosis. Unexpectedly, compound **39f** could also stimulate cell cycle arrest in G1 phase. Further *in vivo* study in WSU-DLCL-2 xenografted mouse model validated the antitumor activities of **27f**, without significant toxicity. The results suggest the therapeutic potential of these HDACs inhibitors in lymphoma and provide valuable insight and understanding for further structural optimisation around *β*-elemene scaffold.
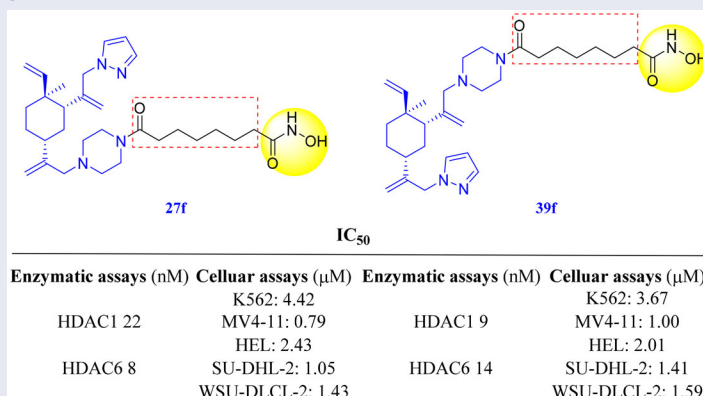
GRAPHICAL ABSTRACT

	IC$_{50}$		
Enzymatic assays (nM)	**Celluar assays** (µM)	**Enzymatic assays** (nM)	**Celluar assays** (µM)
	K562: 4.42		K562: 3.67
HDAC1 22	MV4-11: 0.79	HDAC1 9	MV4-11: 1.00
	HEL: 2.43		HEL: 2.01
HDAC6 8	SU-DHL-2: 1.05	HDAC6 14	SU-DHL-2: 1.41
	WSU-DLCL-2: 1.43		WSU-DLCL-2: 1.59

Introduction

β-Elemene (Figure 1, 1) is a sesquiterpene extracted from the rhizome of *Curcuma wenyujin*[1,2]. It has been used in the treatment of lung cancer, pancreatic cancer, gastric cancer, breast cancer, bladder cancer, and malignant brain glioma[3–8]. Studies have shown that *β*-elemene inhibits tumour cell growth *via* diverse mechanisms[9,10], including induction of apoptosis, autophagy and cell cycle arrest, and inhibition of cell proliferation and migration, etc. However, its clinical application has been limited by poor solubility, low bioavailability, and moderate antitumor activity[11–14]. To overcome these shortcomings, the combination therapy of *β*-elemene with other anticancer drugs, such as cisplatin[15], paclitaxel[16], and gefitinib[17] have been extensively studied. On the other hand, the structural modifications based on *β*-elemene scaffold such as the hydroxyl carboximates derivatives[18], vinylated derivatives[19], *NO*-donating derivatives[20] and macrocycles derivatives[21] have been a major trend for identifying new chemical entities with better anticancer effects and potential better druggability than *β*-elemene. The above mentioned cancer treatment paradigms have achieved great success and broad prospects in the treatment of solid tumours, but has poorly reported for the treatment of lymphoma.
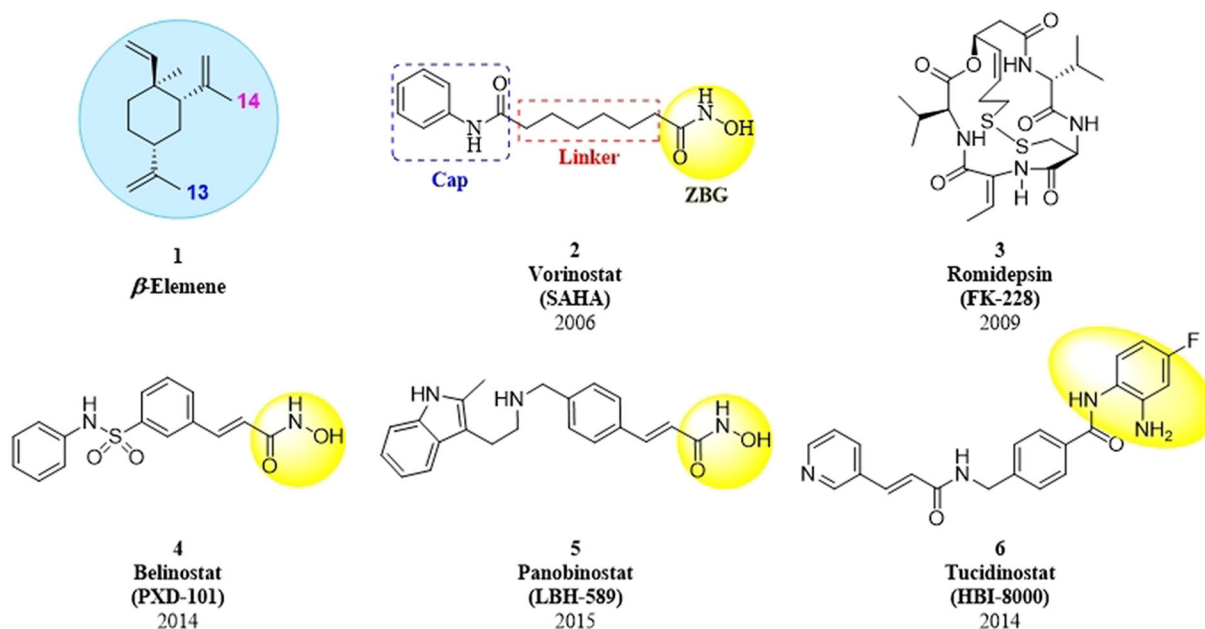
Figure 1. The structures of β-elemene (**1**) and approved HDAC inhibitors (**2–6**).

Histone deacetylases (HDACs) are a family of enzymes that catalyse the deacetylation of lysine residues of both histone and non-histone protein substrates[22,23]. The expression levels of HDACs are usually higher in tumour cells than in normal cells[24]. Inhibition of HDACs can lead to pleiotropic effects on cellular signalling and transcription, including cell death, differentiation, autophagy, and enhancement of immunogenicity[25–30]. To date, five drugs are approved for the treatment of various types of haematologic malignancies: vorinostat (SAHA, **2**), romidepsin (FK-228, **3**), belinostat (PXD-101, **4**), panobinostat (LBH-589, **5**), and tucidinostat (HBI-8000, **6**), as shown in Figure 1. These HDAC inhibitors demonstrated excellent antitumor effect, but generally limited by a narrow antitumor spectrum, drug resistance, and undesirable side effects[31–35]. To address these issues, HDAC inhibitors are clinically used in combination with other antitumor agents to achieve synergistic or additive effects and reduce the potential for developing drug resistance[36–38]. Although drug combinations have the advantages of higher antitumor efficacy, they also suffer from enhanced adverse effects, unpredictable pharmacokinetic profiles, drug-drug interactions, and poor patient compliance[36]. In recent years, the designed and synthesised hybrid drugs, comprising the HDAC inhibitor (HDACi) pharmacophores, are emerging as an alternative strategy to drug combinations[24,39]. Scientific studies have shown that many hybrid agents had more potent anti-proliferation effects than the corresponding single agent[40–45], which encouraged and promoted us to develop the hybrid molecules of β-elemene and HDAC inhibitor.

Based on the above information and our experience in the structural modification of β-elemene, we have designed and synthesised novel HDAC inhibitors derived from the β-elemene scaffold. Herein, we reported the design, synthesis and biological evaluation of the novel HDACi derived from the β-elemene scaffold.

Results and discussion

Design

Generally, the pharmacophores of HDACi are divided into three key components: the cap group (acts as a surface binding, Cap), the linker, and the pharmacophore (zinc-binding group, ZBG) (**2**, Figure 2). The cap portion, which accounts for the affinity gain through hydrophobic interaction with protein, can be large or small in size and can tolerate diverse structures. We envisioned that the lipophilic antitumor β-elemene scaffold should be well tolerated as a cap portion and might potentially provide some beneficial effects to achieve better anticancer activity through "hybrid" drug concept (Figure 2). The linker is typically linear and hydrophobic as well (e.g. straight carbon chain, *trans*- di-substituted olefin or di-substituted phenyl or heteroaryl are often used as the linker). In this study, the different carbon atoms "alkyl linker" and "aromatic linker" was used as the "Linker" to connect the β-elemene derivatives and the "ZBG" portion. The "ZBG" group (also known as pharmacophore or warhead) of many HDACi is hydroxamic acid, and those of few HDACi can also be acyl aniline, cyclic tetrapeptides, thiol, and aliphatic carboxylic acids, or their isosteric replacements. In this work, we examined three common pharmacophores as "ZBG": hydroxamic acid, acyl aniline and acyl pyridine. As a result, six series of HDACi derived from β-elemene scaffold were designed and synthesised, and their biological activities were evaluated.

Chemistry

The synthesis of target compounds **18a–f** and **20** is illustrated in Scheme 1. Bromination between the starting material β-elemene (**1**) and *N*-bromosuccinimide (NBS) yielded 13-Br-β-elemene (**7**). The reaction of **7** with different amines gave *N*-Boc protected intermediates **10a–b**. The Boc protecting group was subsequently removed to yield amines **11a–b**. Separately, the condensation between various carboxylic acids **12a–c** and *O*-(Tetrahydro-2*H*-pyran-2-yl)hydroxylamine (NH₂OTHP) afforded THP-protected intermediates **13a–c**, which underwent ester hydrolysis to give corresponding acids **14a–c**. Then, the amide coupling reaction between amines **11a–b** and carboxylic acids **14a–c** gave intermediates **17a–f**, which underwent subsequent THP deprotection to afford the desired compounds **18a–f**. On the other hand, intermediate **16** was easily obtained from commercially available acyl chloride **15** and NH₂OTHP. The SN₂
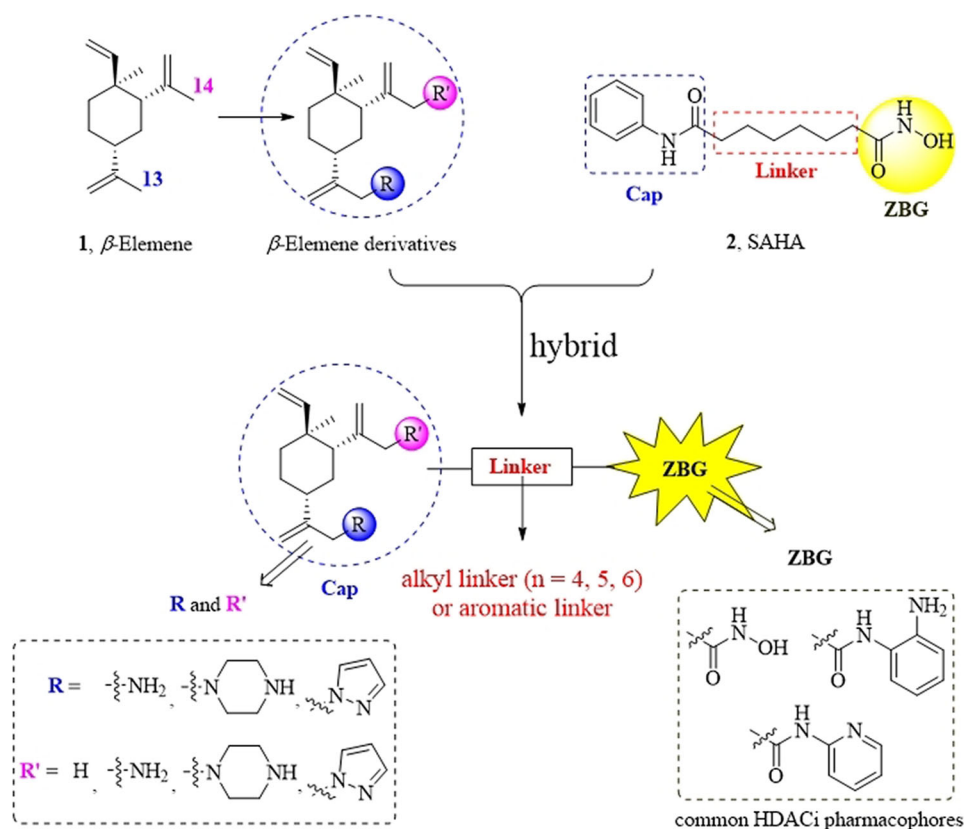
Figure 2. The designing strategy of HDACi derived from β-elemene scaffold.

displacement reaction between **11b** and **16** was facilitated in the presence of DIPEA under heating to afford intermediate **19**, which underwent THP deprotection to give the target compound **20**.

The preparation of analogues **27a–f**, **31–32** and **34** is outlined in Scheme 2. First, β-elemene (**1**) was treated with NaClO under the mixed solvent of AcOH and CH$_2$Cl$_2$ to furnish 13,14-dichloro-β-elemene (**21**). It was discovered by us that the two allylic chloro groups had differentiated reactivity in the presence of a nucleophile. This is presumably due to the stereo effects in the chair-like conformation of cyclohexane ring, in which slightly more bulky around 14-position in **21** leads to less reactivity than 13-position[46]. By carefully controlling the reaction conditions, two different R^3 were installed at position 13- of **21** to yield intermediate **22**. Subsequently, a pyrazole group was installed at position 14- to afford intermediate **24**. The removal of Boc-deprotecting group afforded key intermediates **25a–b**. The transformation of **25a–b** to the target molecules **27a–f** could then be achieved using the similar reaction sequences described in Scheme 1. For the target molecules bearing HDACi pharmacophores other than hydroximate (i.e. **31** and **32**), slightly modified reaction sequence was adopted. Finally, compound **34** was prepared using the similar procedure for compound **20** described in Scheme 1.

Analogues **39a–f**, **41** and **43** were designed to examine the anticancer activity of different attaching positions in comparison with compounds **27a–f**, **31–32**, and **34**. The synthetic route for preparing these compounds is depicted in Scheme 3. The reactions used are similar to those discussed in Scheme 2, except some of the sequences were reversed.

Biological evaluation

In vitro *HDAC inhibition assay*

With several different series of target molecules in hand, assays to evaluate enzymatic inhibitions against HDAC were established. Among all HDAC subtypes, HDAC1 and HDAC6 represent Class I and II, respectively. Small molecules inhibiting both HDAC1 and HDAC6 are typically considered as pan-HDAC inhibitors. On the other hand, when the inhibitors have higher activity against HDAC6 than HDAC1, they are considered as HDAC6-selective inhibitors. Therefore, HDAC1 and HDAC6 were selected for the evaluation of the target molecules (Table 1). Most of the compounds showed moderate to excellent inhibitory activities against HDAC1 and HDAC6. For the compounds bearing alkyl linkers and hydroxamic acid as "ZBG" (i.e. **18a–f**, **27a–f** and **39a–21f**), the length of alkyl linker had a great influence on the HDAC1 and HDAC6 inhibitory activities. For instance, four methylene linker analogs (**18a**, **18d**, **27a**, **27d**, **39a** and **39d**) had poor HDAC1 and HDAC6 inhibitory activities. As the linker length increased, the activities of target molecules improved gradually (**18c** ≈ **18b** > **18a**, **18f** > **18e** > **18d**, **27c** > **27b** > **27a**, **27f** > **27e** > **27d**, **39c** > **39b** > **39a** and **39f** > **39e** > **39d**). Interestingly, compounds with aromatic linkers (i.e. **20**, **34** and **43**) are potent HDAC6-selective inhibitors with 20–64-fold selectivity over HDAC1 (351 nM ≤ IC$_{50}$ ≤ 1120 nM for HDAC1; 11 nM ≤ IC$_{50}$ ≤ 55 nM for HDAC6). It's known that HDAC6-selective inhibitors could have potential therapeutic benefits for lower toxicity and side effects[23], which is worth further investigation in the future.

Subsequently, the influence of the different "Cap" groups on the inhibitory activities of HDAC was evaluated. When
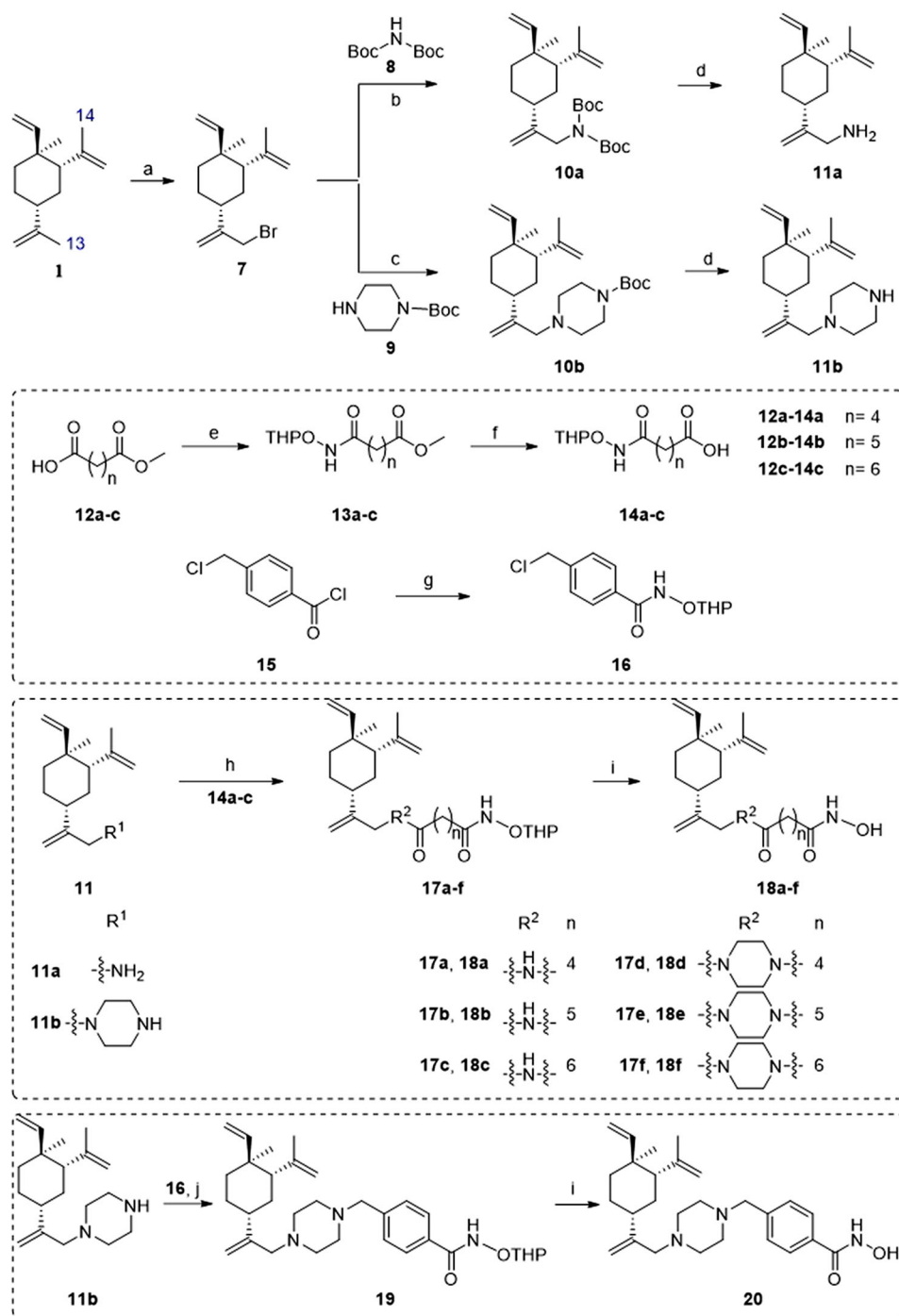
Scheme 1. Synthetic routes of the title compounds **18a–f** and **20**. Reaction conditions and reagents: (a) NBS, AcOH, CH$_2$Cl$_2$, 0 °C to rt, 9 h; (b) Cs$_2$CO$_3$, DMF, Bis(tert-butoxycarbonyl)amine, 60 °C, 10 h; (c) DIPEA, DMF, 1-Boc-piperazine, 60 °C, 10 h; (d) CF$_3$CO$_2$H, 0 °C ∼ rt, 5 h; (e) EDCI, HOBT, DIPEA, DMF, NH$_2$OTHP, rt, 5 h; (f) NaOH (aq), CH$_3$OH, rt, 2 h; (g) CH$_2$Cl$_2$, NH$_2$OTHP, 0 °C, 3 h; (h) EDCI, HOBT, DIPEA, DMF, rt, 5 h; (i) TsOH·H$_2$O, CH$_3$OH, rt, 8 h; (j) DIPEA, DMF, **16**, 60 °C, 6 h.

compounds had the identical "Linker" and "ZBG" group, the following phenomena were observed: (1) Compounds using **11a** as the "Cap" group exhibited better inhibitory activities against HDAC1 and HDAC6 than those compounds using **11b** as the "Cap" group (**18a–c** vs **18d–f**). (2) Compounds using **25a** as "Cap" group exhibited comparable inhibitory activities against HDAC1 and HDAC6 compared to those compounds using **25b** as the "Cap" group. The above two series have one common point the pharmacophore and the linker were attached to the 13-position of β-elemene. On the other hand, when the pharmacophore and the linker attached to the 14-position of β-elemene,

the structure-activity relationships (SARs) were varied from case to case. For instance, compound **39a** using **37a** as the "Cap" group showed 5-fold more potent against HDAC1 and HDAC6 than **39d**. Both **39a** and **39d** had identical aliphatic linkers, i.e. four methylenes length. For other aliphatic linkers such as five or six methylenes length linkers, the trend was reversed, i.e. the activities for **39b–39c** were slightly weaker than that for **39e–39f** (i.e. **39b–39c**, IC$_{50}$ ≤ 136 nM for HDAC1/6; **39e–39f**, IC$_{50}$ ≤ 70 nM for HDAC1/6). Overall, the "Cap" group variation had minimal impact on the inhibitory activities of HDAC.
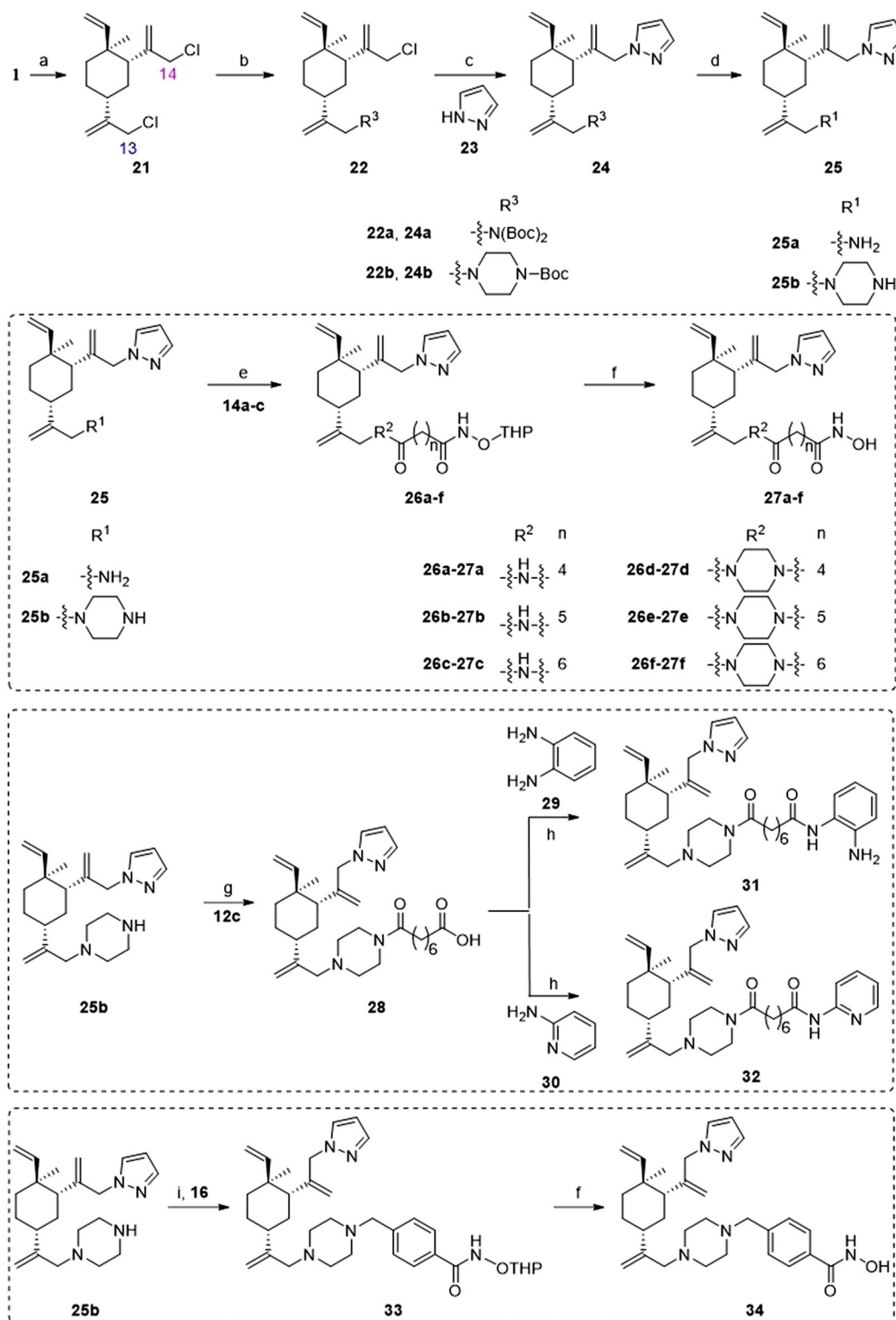
Scheme 2. Synthetic routes of the title compounds **27a–f**, **31–32** and **34**. Reaction conditions and reagents: (a) NaClO, AcOH, CH$_2$Cl$_2$, TBAF, 0 °C, 6 h; (b) Cs$_2$CO$_3$, DMF, **8** or **9**, 50 °C, 8 h; (c) Cs$_2$CO$_3$, DMF, **23**, 60 °C, 10 h; (d) HCl-Dioxane (4 M), rt, 8 h; (e) EDCI, HOBT, DIPEA, DMF, **14a–c**, rt, 5 h; (f) TsOH·H$_2$O, CH$_3$OH, rt, 8 h. (g) (i) EDCI, HOBT, DIPEA, DMF, **12c**, rt, 5 h; (ii) NaOH (aq), CH$_3$OH, rt, 2 h; (h) EDCI, HOBT, DIPEA, DMF, rt, 5 h; (i) DIPEA, DMF, **16**, 60 °C, 6 h.

We further investigated the effects of the "ZBG" group on the inhibitory activities of HDAC. The result suggested that target compounds with hydroxamic acid as the "ZBG" group had better HDAC inhibitory potency than those with o-phenylenediamine or o-aminopyridine as the "ZBG" group. In fact, compounds **31**, **32**, and **41** all have micromole range IC$_{50}$ values indicating weak inhibitory activity against HDAC1 and HDAC6.

After the completion of the evaluation for HDAC enzymatic activity of all compounds, SARs were developed and summarised in Figure 3. To sum up, (1) The "Cap" group, bearing different R and R′ group, had no dramatic influence on HDAC inhibitory activities; (2) Proper linker length was significant for retaining HDAC inhibitory activities and the target compounds with linker length five or six methylene groups appeared to be optimal for obtaining
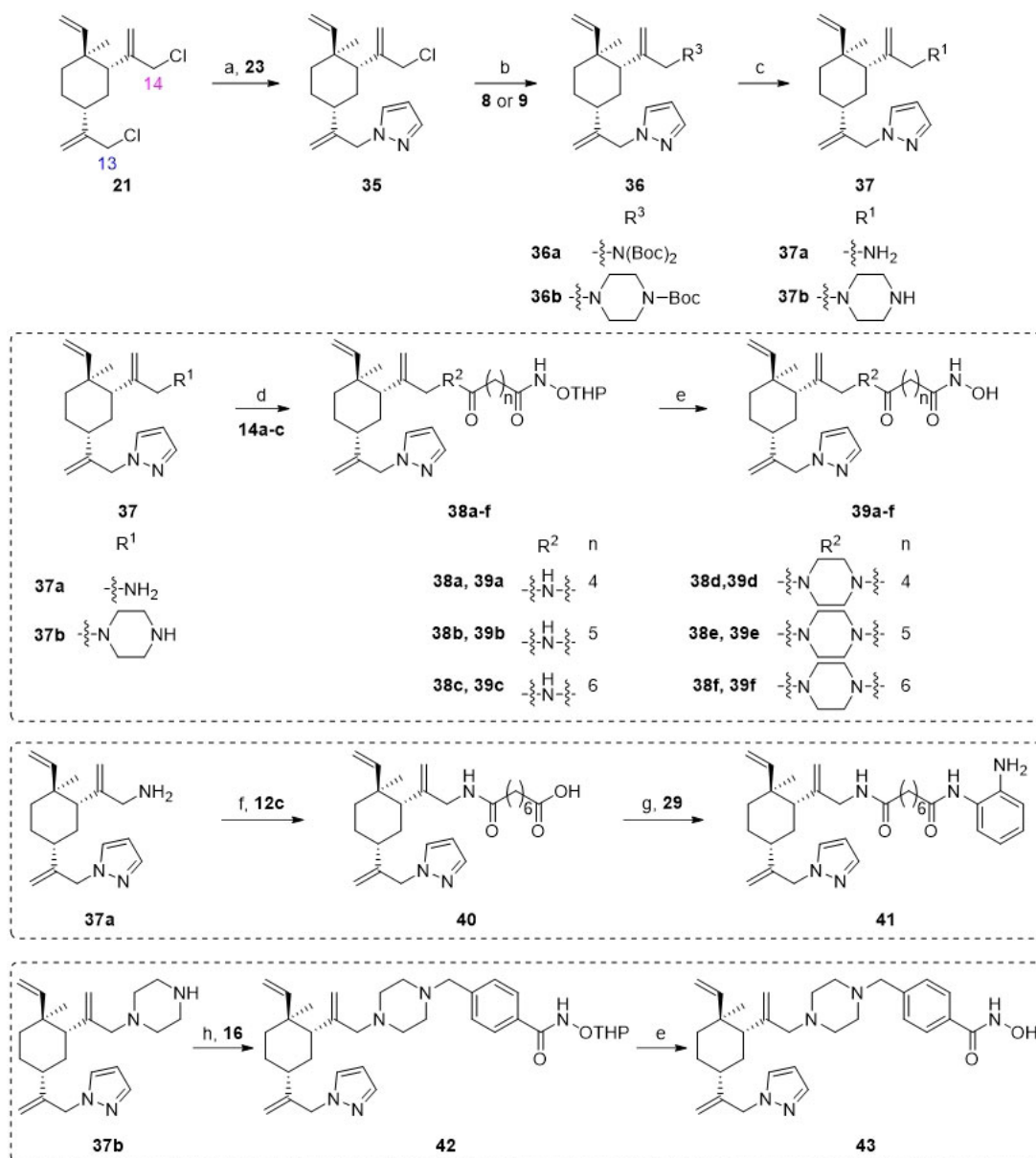
Scheme 3. Synthetic routes of the title compounds **39a–f**, **41** and **43**. Reaction conditions and reagents: (a) Cs_2CO_3, DMF, **23**, 45 °C, 10 h; (b) Cs_2CO_3, DMF, **8** or **9**, 80 °C, 8 h; (c) HCl-Dioxane (4 M), rt, 8 h; (d) EDCI, HOBT, DIPEA, DMF, **14a–c**, rt, 5 h; (e) TsOH·H_2O, CH_3OH, rt, 8 h; (f) (i) EDCI, HOBT, DIPEA, DMF, **12c**, rt, 5 h; (ii) NaOH (aq), CH_3OH, rt, 2 h; (g) EDCI, HOBT, DIPEA, DMF, **29**, rt, 5 h; (h) DIPEA, DMF, **16**, 60 °C, 6 h.

potent inhibitory activities against HDAC; (3) The compounds bearing aromatic structures as a part of the linker showed up to 64-fold HDAC6-selectivity over HDAC1; (4) "Hydroxamic acid" appears to be the best "ZBG" group than others such as "o-amino-pyridine" and the "o-phenylenediamine".

In vitro anti-proliferative assay

Compounds with good activities against HDAC1 ($IC_{50} \leq 53$) and HDAC6 ($IC_{50} \leq 15$ nM) were selected to perform anti-proliferative activities experiment against three different leukaemia cells (K562, MV4-11 and HEL cells) using the standard CCK8 test method (Table 2). The results suggested that compounds **18b**, **27c**, **27f** and **39f** were potent in inhibiting the proliferation of three types of leukaemia cells. Among all compounds tested against MV4-11 cell proliferation, **27f** showed the best cytotoxicity with an IC_{50} value of 0.79 μM, which was over 250-fold more potent than

β-elemene. The IC_{50} values for compounds **18b**, **27c** and **39f** were all less than 1.65 μM. To further identify whether these four molecules had broad-spectrum antitumor activities, we determined their inhibitory activities against two other lymphoma cells: SU-DHL-2 and WSU-DLCL-2 (Table 2). Strikingly, the anti-proliferative activities of compounds **18b**, **27c**, **27f** and **39f** against SU-DHL-2 cell were < 1.55 μM, which was significantly superior to compounds **1** ($IC_{50} > 200$ μM) and **2** ($IC_{50} = 1.84$ μM). For WSU-DLCL-2 cells, these four compounds displayed over 88-fold more potent than their parent β-elemene. The above results suggested that (1) The anti-proliferative activities of the combination drug were stronger than that of β-elemene and SAHA alone, which was consistent with our expectation; (2) Compared with their parent β-ele-mene, our tested compounds showed more potent anti-proliferative activities against five cell lines; (3) The anti-prolifer-ation activities of **27f** were comparable with those of **39f** and slightly stronger those of **18b** and **27c** in all tested tumour cells.

Table 1. The structures and corresponding IC$_{50}$ values of the target compounds against HDAC1 and HDAC6.
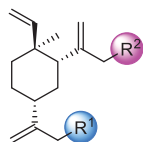
Compd.	R^1	R^2	IC$_{50}$ (μM) HDAC1[a,b]	IC$_{50}$ (μM) HDAC6[a,b]
18a		H	0.567 ± 0.043	0.193 ± 0.022
18b		H	0.041 ± 0.006	0.010 ± 0.003
18c		H	0.056 ± 0.012	0.009 ± 0.001
18d		H	0.900 ± 0.078	0.532 ± 0.027
18e		H	0.461 ± 0.066	0.039 ± 0.013
18f		H	0.081 ± 0.008	0.032 ± 0.009
20		H	1120 ± 0.072	0.055 ± 0.002
27a			0.879 ± 0.056	0.261 ± 0.004
27b			0.061 ± 0.013	0.021 ± 0.007
27c			0.053 ± 0.011	0.015 ± 0.005
27d			0.858 ± 0.045	0.522 ± 0.081
27e			0.189 ± 0.026	0.032 ± 0.006
27f			0.022 ± 0.004	0.008 ± 0.001
31			> 5.0	> 5.0

(continued)

Table 1. Continued.

Compd.	R¹	R²	IC₅₀ (μM) HDAC1[a,b]	IC₅₀ (μM) HDAC6[a,b]
32			3.544 ± 0.195	> 5.0
34			0.351 ± 0.037	0.012 ± 0.002
39a			0.986 ± 0.013	0.398 ± 0.041
39b			0.136 ± 0.033	0.020 ± 0.007
39c			0.050 ± 0.003	0.021 ± 0.005
39d			> 5.0	> 5.0
39e			0.070 ± 0.008	0.024 ± 0.004
39f			0.009 ± 0.004	0.014 ± 0.001
41			2.134 ± 0.294	> 5.0
43			0.710 ± 0.053	0.011 ± 0.006
1	H	H	*N.D.*	*N.D.*
2	—	—	0.018 ± 0.004	0.012 ± 0.001

[a]Assays were performed in replicate ($n > 2$); IC₅₀ values are shown as mean ± SD. [b]*N.D.* means not determined.

Considering the anti-enzyme activities and tumour cell proliferation inhibitory activities, we finally chose compounds **27f** and **39f** as the representative compounds for follow-up research.

The solubility and solubility levels predictions of the selected compounds

Accelrys Discovery Studio (DS) software was used to assess the solubility level of target compounds (Table 3). The results suggested that compounds **18b**, **27c**, **27f** and **39f** were expected to have better aqueous solubility compared to the β-elemene group. Compounds **27f** and **39f** are slightly better than **18b** and **27c**.

In vitro induced cell apoptosis

Based on inhibitory activities against HDAC1 and HDAC6, antiproliferative activities against tumour cells, and calculated aqueous solubility level, compounds **27f** and **39f** were selected for further studies on their pro-apoptotic activity using flow cytometry (Figure 4). Compounds **27f** and **39f** exhibited same magnitude of activity in the five cancer cell lines tested above. Since WSU-DLCL-2 is one of aggressive forms of diffuse large B-cell lympoma (DLBCL) with fewer effective treatment option, it was selected for flow cytometry. The results indicated that the ability of compounds **27f** and **39f** to induce WSU-DLCL-2 cells apoptosis at the concentration of 5 μM was comparable to SAHA, but was significantly stronger than β-elemene. Interestingly, SAHA possessed a certain level of synergistic pro-apoptotic effects when combined with β-elemene at the concentration of 5 μM (the percentage of cell apoptosis: 49.01%, 79.12%, and 87.09%, β-elemene, SAHA, and β-elemene + SAHA (1:1) respectively). Intriguingly, compounds **27f** and **39f** could significantly induced WSU-DLCL-2 cell apoptosis. Compound **27f**, in particular, showed a much higher apoptosis rate at 10 uM than at 5 uM (91.57% vs 77.05%) in a dose-dependent manner. The above results indicated that compounds **27f** and **39f** could effectively induce WSU-DLCL-2 cell apoptosis, which are more potent than β-elemene.
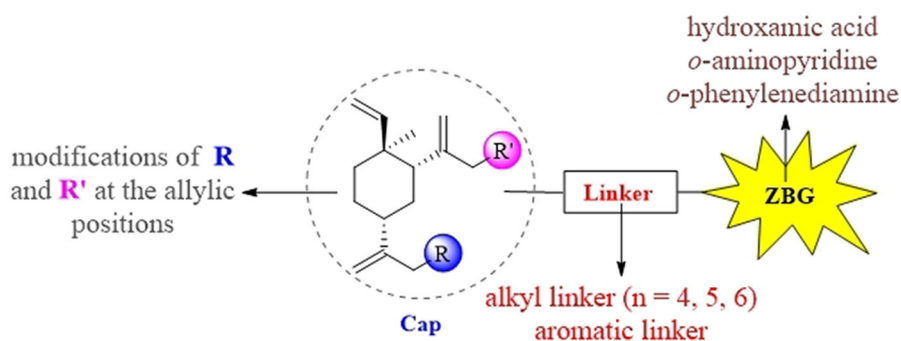
Figure 3. SARs summary of histone deacetylase inhibitors derived from β-elemene scaffold.

Table 2. *In vitro* anti-proliferative evaluation of target compounds against selected cell lines.

	IC$_{50}$ (μM)[a]				
	Leukaemia cell lines			Lymphoma cell lines	
Compound	K562	MV4-11	HEL	SU-DHL-2	WSU-DLCL-2
18b	5.16 ± 0.13	1.28 ± 0.11	2.16 ± 0.16	1.52 ± 0.13	2.08 ± 0.22
27c	5.60 ± 0.04	1.63 ± 0.09	6.05 ± 0.24	1.31 ± 0.18	2.27 ± 0.30
27f	4.42 ± 0.56	0.79 ± 0.15	2.43 ± 0.09	1.05 ± 0.09	1.43 ± 0.15
39f	3.67 ± 0.50	1.00 ± 0.05	2.01 ± 0.27	1.41 ± 0.04	1.59 ± 0.42
1	> 200	> 200	> 200	> 200	> 200
2	1.70 ± 0.01	< 0.37	0.60 ± 0.02	1.84 ± 0.21	1.37 ± 0.09
1 + 2 (1:1)	1.61 ± 0.13	< 0.37	0.43 ± 0.15	0.96 ± 0.05	1.19 ± 0.12

[a]Assays were performed in replicate ($n > 2$); IC$_{50}$ values are shown as mean $\pm$ SD.

Table 3. The solubility and solubility levels predictions of the selected compounds.

Compound	ADMET solubility	ADMET solubility level
18b	-3.342 ↑	3 ↑
27c	-3.373 ↑	3 ↑
27f	-3.311 ↑	3 ↑
39f	-3.273 ↑	3 ↑
1	-5.393	2

In vitro *arrested cell cycle*

In addition to studying the effects of compounds **27f** and **39f** on cell apoptosis, we also explored their effects on cell cycle progression by flow cytometry. As shown in Figure 5, DMSO, β-elemene, SAHA and β-elemene + SAHA were used as the blank and positive control, respectively. WSU-DLCL-2 cells were treated with compounds **27f** and **39f** at 1 μM and 5 μM for 72 h, respectively. The results revealed that β-elemene, SAHA, β-elemene + SAHA, **27f** and **39f** groups had hardly or slight effects on cell cycle at 1 μM. When the concentration of compound **27f** was increased to 5 μM, the cell proportion of G1, G2 and S phase did not significantly change, compared with the control group and **27f** group at 1 μM. However, the cell proportion of G1 phase increased dramatically (G1: 54.55% *vs* 70.18%) and the cell proportion of S phase and G2 phase decreased accordingly (S: 37.21% *vs* 27.83%; G2: 7.07% *vs* 1.31%), when the concentration of compound **39f** was increased from 1 μM to 5 μM. The above results indicated that compound **39f** could arrest the WSU-DLCL-2 cell cycle at the G1 phase in a concentration-dependent manner.

Molecular docking study

To better understand the binding modes of compounds **29f** and **39f** with HDAC1, and HDAC6, we performed molecular docking studies using the solved crystal structures of hHDAC1[47] (PDB ID 5ICN) and hHDAC6[48] (PDB ID 5EDU), as shown in Figure 6(A–D). Compounds **27f** and **39f** bound with HDAC, mainly through formed metal-acceptor bonding interactions with zinc ions and hydrogen bonds interactions with amino acid residues on the surface of HDAC. In studying the molecular docking of compounds **27f** and **37f** with the active pocket of HDAC1, it was found that both **27f** and **37f** could form metal-acceptor bonding interactions with Zn^{2+}. The difference is that **27f** formed three hydrogen bonds with D99, H178 and G301, respectively (Figure 6(A)). In comparison, **39f** formed five hydrogen bonds with R270, L271, H178, D176 and H140, respectively (Figure 6(C)). This may be the reason that compound **27f** had a slightly weaker inhibitory activity against HDAC1 than **39f**. A similar phenomenon was observed in the molecular docking analysis of **27f** and **39f** in the active pocket of HDAC6. The hydroxamic acid moiety of **27f** and **39f** were stretched into the catalytic pocket, forming a coordination contact with Zn^{2+}. The difference is that **27f** formed interaction with H499 and Y782 respectively (Figure 6(B)), while **39f** formed interactions with S568 (Figure 6(D)). This may be the reason that compound **27f** displayed more potent inhibitory activity against HDAC6 than **39f**. The docking results proposed the favourable binding mode of our synthesised HDAC inhibitors **27f** and **39f** and explained their good inhibitory activities against HDAC1 and HDAC6.

Oral pharmacokinetics study

Due to its excellent HDAC inhibitory activities, potent anti-proliferative and pro-apoptosis capacities and good solubility level, compound **27f** was progressed into an *in vivo* pharmacokinetic (PK) study. Compound **27f** was administered intravenously (*i.v.*) at 5 mg/kg or orally (*p.o.*) at 10 mg/kg to female ICR mice. As shown in Table 4, **27f** was rapidly cleared with the clearance (CL) of 65.1 ml/(h·kg) and the half-life (T$_{1/2}$) of 0.361 h, after intravenous administration. The oral bioavailability of **27f** was low (3.15%), presumably due to the rodent-specific PK profiles of HDACs pharmacophore (similar to SAHA). These data suggested that oral administration was not a suitable dosing route for compound **27f**.

In vivo *antitumor activity against WSU-DLCL2 xenografts*

In a proof of concept study, **27f** was intraperitoneally administrated to WSU-DLCL-2 xenografted mice model to preliminarily evaluate its *in vivo* antitumor potency. First, WSU-DLCL-2 cells (4×10^6) were implanted in the right flanks subcutaneously in female nude mice. When the implanted tumour reached a volume of $100 \sim 150$ mm^3, the animals were randomly divided into groups of 2. In one of the groups, animals were treated with compound **27f** intraperitoneally at 50 mg/kg once a day (QD) for 21 consecutive days. In another group, animals were treated with vehicles. As
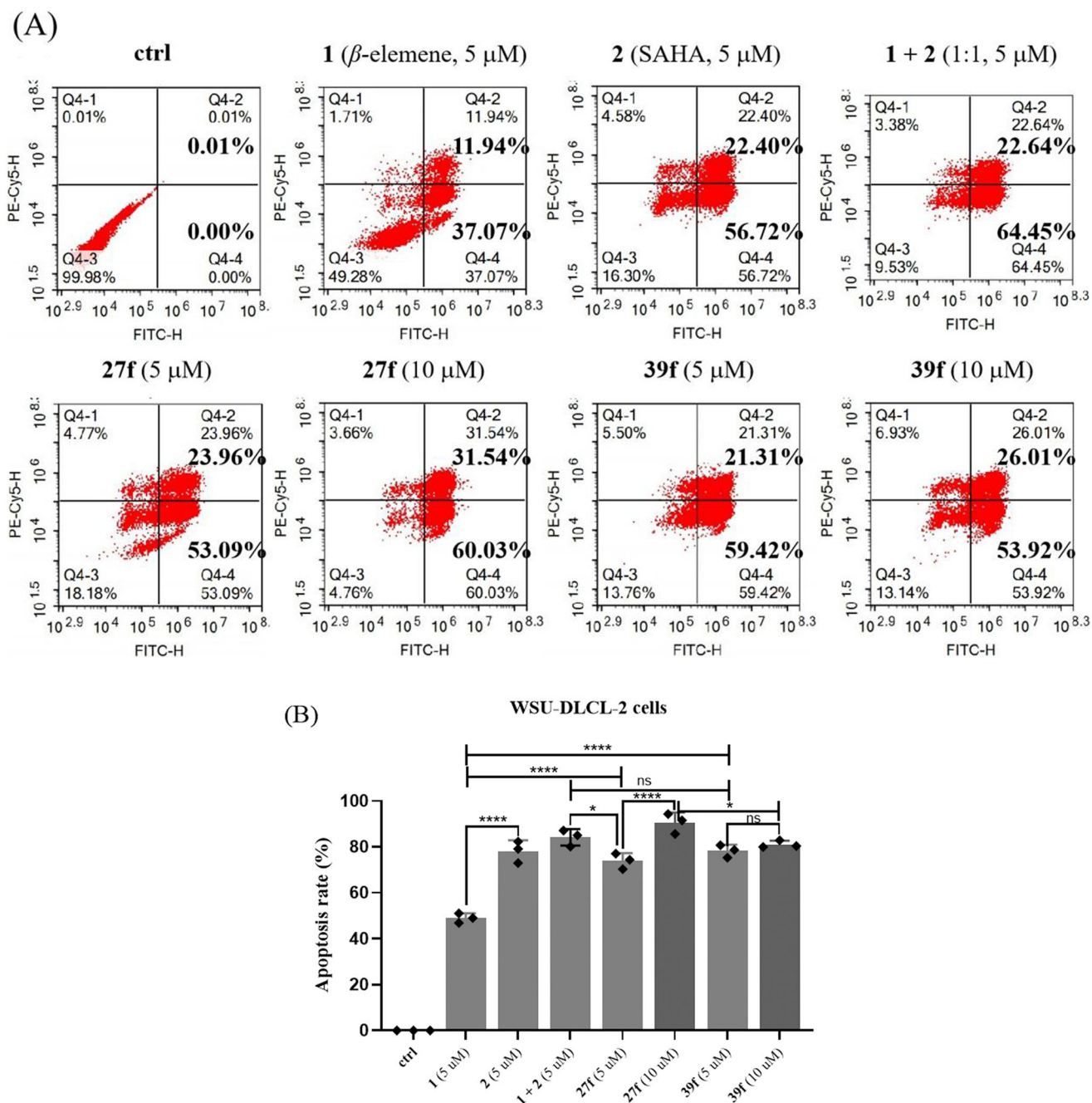
Figure 4. Effects of compounds **27f** and **39f** on cell apoptosis. (A) WSU-DLCL-2 cells were treated with 5 μM and 10 μM of compounds **27f** and **39f** for 72 h. Cells treated with DMSO were used for comparison and cells treated with **1**, **2** and **1 + 2** (1:1) were used for positive control. Data were represented as mean standard deviation from three independent experiments; (B) The histogram of compounds **1**, **2**, **1 + 2** (1:1), **27f** and **39f** on WSU-DLCL-2 cells apoptosis. Data are expressed as the mean ± SD ($n = 3$). $*p < 0.05$, $**p < 0.01$, $***p < 0.001$ by one-way ANOVA test and Turkey's comparison test, ns: not statistically.

shown in Figure 7, **27f** showed a moderate *in vivo* antitumor potency with TGI of 31.5%. The tumour growth curve and the final tumour tissue size are presented in Figure 7(A,C), respectively, which explicitly demonstrates the superior *in vivo* potency of compound **27f** group.

Conclusion and discussion

To improve antitumor activities of β-elemene and expand its scope of clinical application, we designed and synthesised a novel series of novel HDACi based on β-elemene structure in this study. Most of the prepared compounds exhibited potent inhibitory

activities against HDACs and significant inhibitory effects on the proliferation of K562 and MV4-11. In particular, the representative compounds **27f** and **39f** demonstrated excellent *in vitro* anti-enzyme (IC$_{50}$ values of 22 nM and 9 nM for HDAC1 and 8 nM and 14 nM for HDAC6, respectively) and broad spectrum *in vitro* anti-proliferative activities (IC$_{50}$ values ranging from 0.79 to 4.42 μM against K562, MV4-11, HEL, SU-DHL-2 and WSU-DLCL-2 cell lines). Preliminary mechanistic studies revealed that compounds **27f** and **39f** could efficiently induce cell apoptosis. Unexpectedly, compound **39f** could also stimulate cell cycle arrest in G1 phase. Further *in vivo* study in WSU-DLCL-2 xenograft mouse model validated the antitumor activities of **27f**, without significant toxicity.
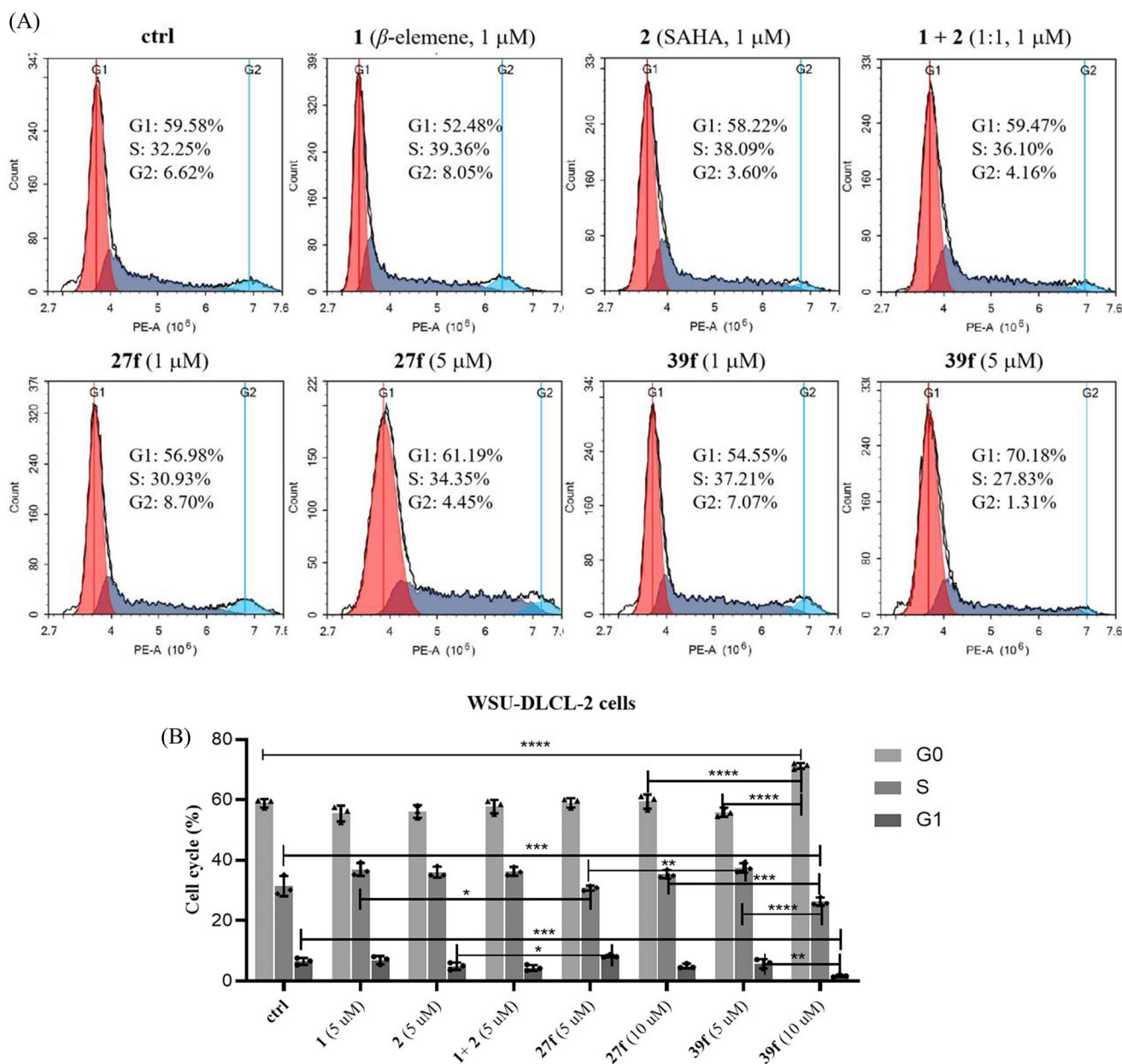
Figure 5. Effects of compounds **27f** and **39f** on cell cycle. (A) WSU-DLCL-2 cells were treated with 1 μM and 5 μM of compounds **27f** and **39f** for 72 h. Cells treated with DMSO were used for comparison and cells treated with **1**, **2** and **1 + 2** (1:1) were used for positive control. Data were represented as mean standard deviation from three independent experiments; (B) The histogram of compounds **1**, **2**, **1 + 2** (1:1), **27f** and **39f** on WSU-DLCL-2 cells cycle. Data are expressed as the mean ± SD ($n = 3$). *$p < 0.05$, **$p < 0.01$, ***$p < 0.001$, ****$p < 0.0001$ by one-way ANOVA test and Turkey's comparison test.

In summary, we have reported a series of novel compounds with potent HDAC inhibitory activity by installing HDACi pharmacophore onto β-elemene scaffold. Despite good progress has been obtained, more work is needed to better understand the SAR and to guide the future structural optimisation. For example, it could be interested to evaluate the compounds against other cancer cell lines including both solid tumour cells and haematologic cells. Further optimisation of lead **27f** could also help to identify compounds with improved oral bioavailability. In addition, in-depth mechanism studies should be done with some of the most potent derivatives to elucidate the pathway and target proteins involved in antitumor effects. Nevertheless, our results reported herein should provide useful information for the future studies in this field.

Experimental section

Chemistry

General information

All of the chemical materials were purchased from commercial suppliers. The melting points of the compounds were determined using Büchi B-540 capillary melting point instrument. NMR spectra were recorded on a Bruker instrument at 400 MHz for ^{1}H NMR and 100 MHz for ^{13}C NMR, using CDCl$_3$, CD$_3$OD or DMSO-d$_6$ as the deuterated solvent. Chemical shifts (δ) were reported in parts per million (ppm) relative to residual solvent as an internal reference. Low-resolution mass spectra were registered with Agilent 1260 InfinityII/6125. High-resolution mass spectra (HRMS) were measured on a Bruker MICR OTOF-Q II instrument.
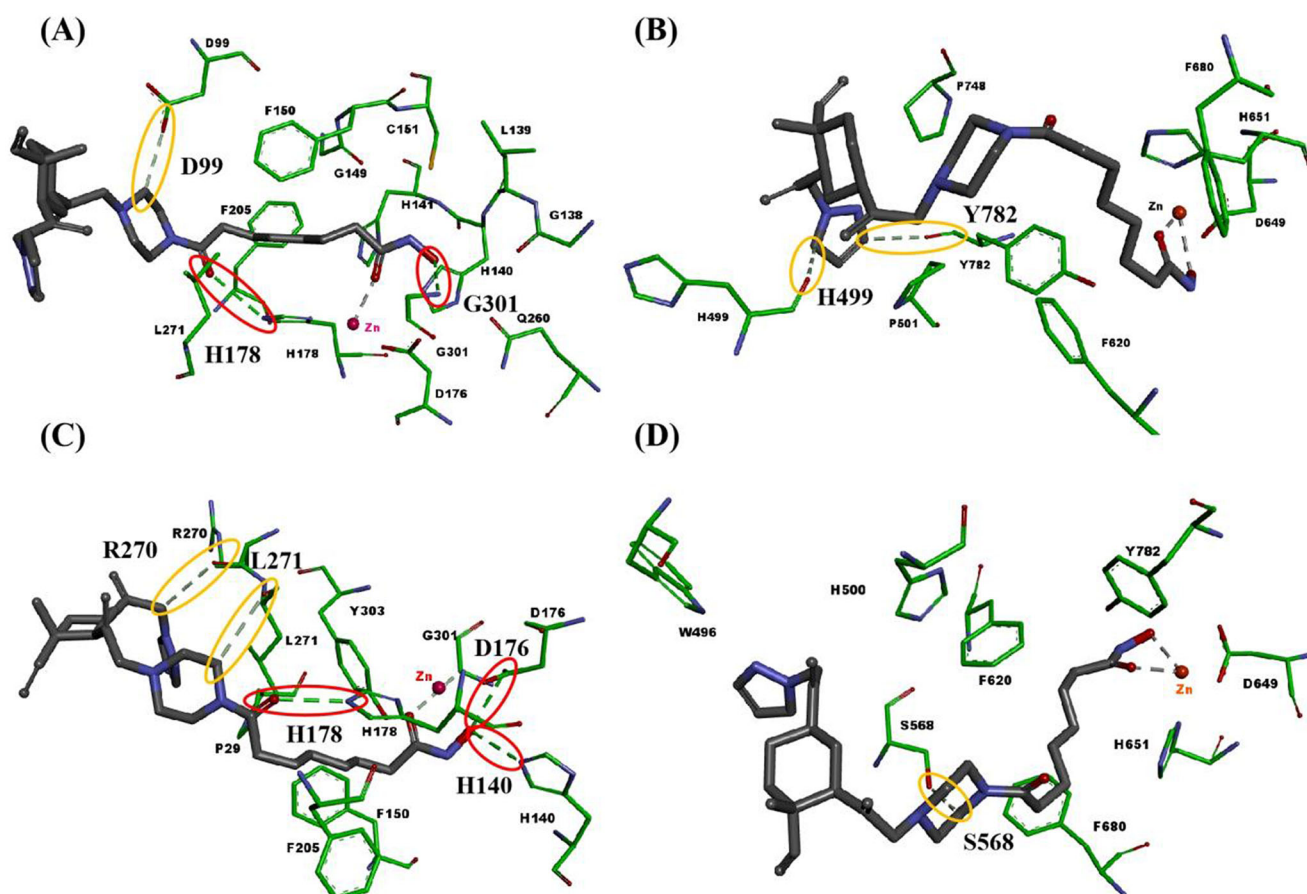
Figure 6. Binding modes of compounds **27f** or **39f** with hHDAC1 (PDB ID 5ICN) and hHDAC6 (PDB ID 5EDU). (A) Binding model of compound **27f** with hHDAC1; (B) Binding model of compound **27f** with hHDAC6; (C) Binding model of compound **39f** with hHDAC1; (D) Binding model of compound **39f** with hHDAC6. Only surrounding amino acid residues are shown for clarity. The zinc ion is representative as red sphere, and hydrogen bonds are indicated with dashed lines. The conventional hydrogen bond is representative as red ellipse. The carbon hydrogen bond is representative as yellow ellipse. The carbons of compounds **27f** and **39f** are coloured in black. The oxygen atoms are coloured in red, and nitrogen atoms in blue.

Table 4. *In vivo* pharmacokinetic properties of **27f**[a].

PK parameters	i.v. (5 mg/kg)	p.o. (10 mg/kg)
$T_{1/2}$ (h)	0.36 ± 0.10	0.88 ± 0.14
T_{max} (h)	—	0.25 ± 0.11
C_{max} (ng/ml)	—	54.70 ± 7.20
AUC_{0-t} (h*ng/ml)	1278.00 ± 253.00	77.80 ± 9.30
AUC_{0-inf} (h*ng/ml)	1279.00 ± 142.00	80.70 ± 13.10
Vz (L/kg)	1.08 ± 0.36	158.00 ± 14.00
CL (ml/min/kg)	65.10 ± 11.22	2066.00 ± 394.00
MRT_{0-inf} (h)	0.28 ± 0.08	1.08 ± 0.17
F(%)		3.15 ± 0.05

[a]All experiments are expressed as the mean ± standard deviation of three separate determinations (mean ± SD).

Synthesis of the crucial intermediate 7. To a solution of β-elemene (**1**, 6.01 g, 29.46 mmol) in AcOH (20 ml) was added *N*-bromosuccinimide (NBS, 6.29 g, 35.35 mmol) at 0 °C. After addition, the mixture was stirred at room temperature for 9 h. The reaction was monitored by TLC. Upon completion, the mixture was then neutralised with saturated aqueous NaHCO₃ solution and extracted with petroleum ether (PE, 3 × 100 ml). The combined organic layers were washed with water and brine, and dried over Na₂SO₄. The drying agent was filtered off. The filtrate was concentrated under reduced pressure, and the residue was purified *via* flash column chromatography (PE as eluent) to give 13-Br-β-elemene **7** (2.51 g, yield 30.1%) as a light yellow liquid. ¹H NMR (400 MHz, CDCl₃) δ 5.89–5.76 (m, 1H), 5.21 (s, 1H), 5.04 (t, $J = 1.1$ Hz, 1H),

4.97–4.81 (m, 3H), 4.59 (*d*t, $J = 1.9$, 0.9 Hz, 1H), 4.04 (*d*, $J = 0.7$ Hz, 2H), 2.33–2.17 (m, 1H), 2.06 (*dd*, $J = 12.6$, 3.5 Hz, 1H), 1.74–1.70 (m, 3H), 1.69–1.39 (m, 6H), 1.01 (s, 3H).

Synthesis of intermediate 10a. A solution of intermediate **7** (1.72 mmol), bis(tert-butoxycarbonyl)amine (**8**, 4.47 mmol) and Cs₂CO₃ (2.58 mmol) in *N,N*-dimethylformamide (DMF, 5 ml) was stirred at 60 °C for 10 h. The reaction was monitored by TLC. Upon completion, the mixture was diluted in H₂O (50 ml) and was extracted with ethyl acetate (EA, 3 × 30 ml). The combined organic layers were washed with water and brine, and dried over Na₂SO₄. The drying agent was filtered off. The filtrate was concentrated under reduced pressure, and the residue was purified *via* column chromatography (PE/EA 4:1, v/v) to give **10a** (575.93 mg, yield 79.8%) as a light yellow liquid.

Synthesis of intermediate 10b. A solution of intermediate **7** (0.40 mmol), 1-Boc-piperazine (0.48 mmol) and DIPEA (0.48 mmol) in DMF (5 ml) was stirred at 60 °C for 10 h. The reaction was monitored by TLC. Upon completion, the mixture was diluted in H₂O (50 ml) and was extracted with EA (3 × 50 ml). The combined organic layers were washed with water and brine, and dried over Na₂SO₄. The drying agent was filtered off. The filtrate was concentrated under reduced pressure, and the residue was purified *via* column chromatography (PE/EA 3:1, v/v) to give **10b** (122.40 mg, yield 78.8%) as a light yellow liquid. ¹H NMR (400 MHz, CDCl₃) δ
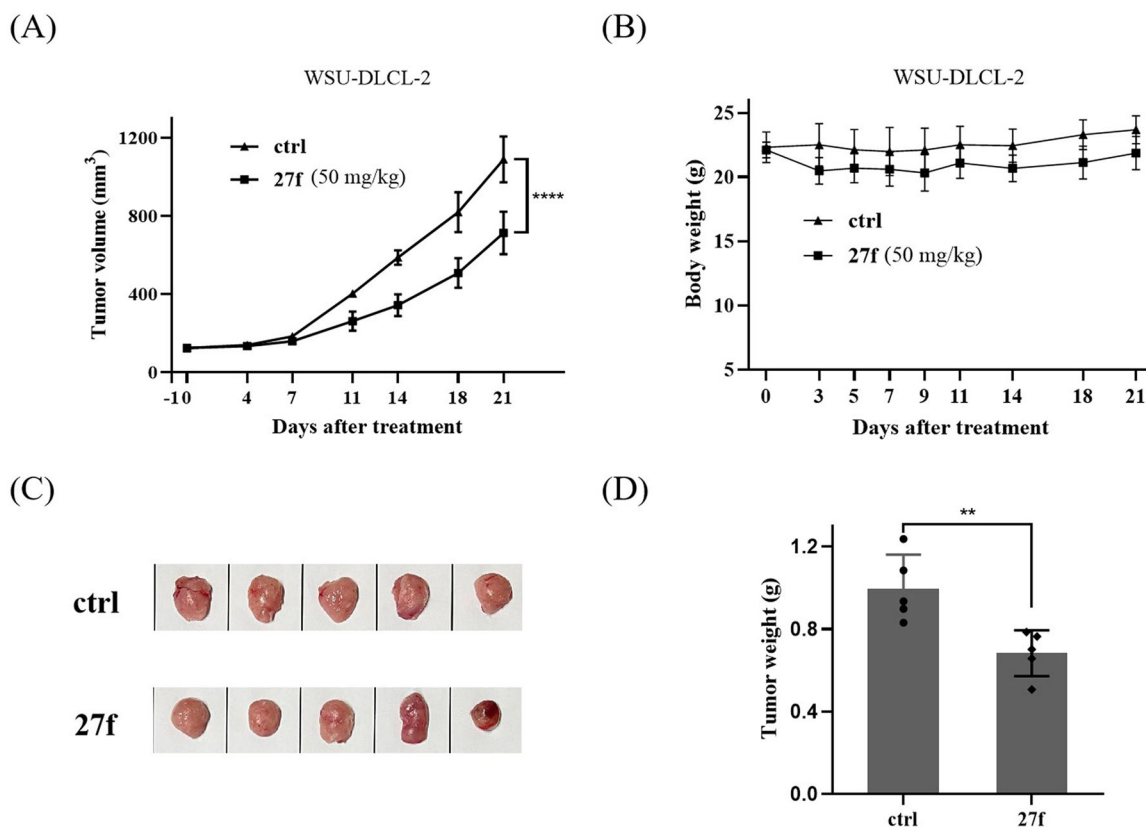
Figure 7. Tumour growth inhibition of compound **27f** in WSU-DLCL-2 xenografted mice model. (A) The efficacy of compound **27f** in the WSU-DLCL-2 xenograft model. (B) Average body weights for **27f** and vehicle-treated mice groups. (C) Photo of dissected WSU-DLCL-2 tumour tissues. (D) Tumour weight of dissected WSU-DLCL-2 tumour tissues. Single asterisks indicate $p < 0.05$, double asterisks indicate $p < 0.01$, and triple asterisks indicate $p < 0.001$ versus the control group. *$p < 0.05$, **$p < 0.01$, ***$p < 0.001$, ****$p < 0.0001$ by two-way ANOVA test.

5.76 (dd, $J = 17.9$, 10.4 Hz, 1H), 4.94–4.77 (m, 4H), 4.77–4.72 (m, 1H), 4.51 (s, 1H), 3.35 (s, 4H), 2.86 (q, $J = 11.6$, 9.8 Hz, 2H), 2.26 (s, 4H), 2.08–1.89 (m, 2H), 1.64 (s, 3H), 1.62–1.40 (m, 6H), 1.39 (s, 9H), 0.94 (s, 3H).

General procedure for the synthesis of intermediate 11. To a solution of intermediate **10** (1.37 mmol) in dichloromethane (DCM, 3 ml) in an ice-cooled bath was slowly added CF_3CO_2H (1.5 ml) solution. The mixture was gradually warmed to room temperature and stirred for 5 h. The reaction was monitored by TLC. Upon completion, the reaction solution was slowly added to the saturated $NaHCO_3$ solution (until no bubbles were formed) at 0 °C. Then the mixture was extracted with EA (3 × 50 ml). The combined organic layers were washed with water and brine, and dried over Na_2SO_4. The drying agent was filtered off. The filtrate was concentrated under reduced pressure, and the residue was directly used in the next reaction without purification.

General procedure for the synthesis of intermediates 13a–c. A solution of $H_2N-OTHP$ (1.63 mmol), DIPEA (4.08 mmol), EDCI (3.54 mmol), HOBt (1.77 mmol) and the corresponding acids (**12**, 1.36 mmol) in DMF (5 ml) was stirred at room temperature for 5 h. The reaction was monitored by TLC. Upon completion, the mixture was diluted in H_2O (50 ml) and was extracted with EA (3 × 50 ml). The combined organic layers were washed with water and brine, and dried over Na_2SO_4. The drying agent was filtered off. The filtrate was concentrated under reduced pressure, and the residue was purified *via* column chromatography (DCM/MeOH 9:1, v/v) to give the products as a colourless liquid.

Methyl 6-oxo-6-(((tetrahydro-2H-pyran-2-yl)oxy)amino)hexanoate (13a). Colourless liquid, yield 81.0%. ^{1}H NMR (500 MHz, $CDCl_3$) δ 8.60 (s, 1H), 4.95 (s, 1H), 4.04–3.87 (m, 1H), 3.67 (s, 3H), 3.66–3.61 (m, 1H), 2.35 (td, $J = 6.7$, 6.2, 3.4 Hz, 2H), 2.18 (d, $J = 30.1$ Hz, 2H), 1.93–1.47 (m, 10H).

Methyl 7-oxo-7-(((tetrahydro-2H-pyran-2-yl)oxy)amino)heptanoate (13b). Colourless liquid, yield 92.0%. ^{1}H NMR (500 MHz, $CDCl_3$) δ 8.48 (s, 1H), 4.94 (s, 1H), 3.95 (s, 1H), 3.67 (s, 3H), 3.66–3.61 (m, 1H), 2.32 (t, $J = 7.5$ Hz, 2H), 2.13 (s, 2H), 1.90–1.78 (m, 3H), 1.73–1.53 (m, 7H), 1.42–1.32 (m, 2H).

Methyl 8-oxo-8-(((tetrahydro-2H-pyran-2-yl)oxy)amino)octanoate (13c). Colourless liquid, yield 86.4%. ^{1}H NMR (400 MHz, $CDCl_3$) δ 8.35 (s, 1H), 4.95 (s, 1H), 3.93 (d, $J = 10.6$ Hz, 1H), 3.67 (s, 3H), 3.66–3.60 (m, 1H), 2.31 (t, $J = 7.4$ Hz, 2H), 2.11 (m, 2H), 1.90–1.73 (m, 3H), 1.67–1.54 (m, 7H), 1.41–1.29 (m, 4H).

General procedure for the synthesis of intermediates 14a–c. A solution of intermediates **13** (1.03 mmol) and cooled NaOH aqueous solution (1 N, 3 ml) in CH_3OH (3 ml) was stirred at room temperature for 2 h. The reaction was monitored by TLC. Upon completion, the mixture was concentrated *in vacuo*. Then the residue was neutralised by HCl solution (1 M) to pH 6 ∼ 7 and was extracted with EA (3 × 20 ml). The organic layer was separated, washed with water and brine, dried over Na_2SO_4. The drying agent was filtered off. The filtrate was concentrated under reduced pressure, and the residue was directly used in the next reaction without purification.

Synthesis of intermediate 16. To a solution of $H_2N-OTHP$ (17.46 mmol) and Et_3N (31.75 mmol) in DCM (15 ml) was added dropwise DCM solution (15 ml) containing compound **15** (15.87 mmol) at $0\,^{\circ}C$. After addition, the mixture was stirred at room temperature for $2\sim3$ h. The reaction was monitored by TLC. Upon completion, the mixture was diluted in H_2O (50 ml) and was extracted with DCM (3×50 ml). The organic layer was separated, washed with water and brine, dried over Na_2SO_4. The drying agent was filtered off. The filtrate was concentrated under reduced pressure, and the residue was purified via column chromatography (PE/EA 3:2, v/v) to give **16** (1.51 g, yield 35.4%) as a white solid. ^{1}H NMR (500 MHz, DMSO-d_6) δ 11.66 (s, 1H), 7.77 (d, $J = 8.2$ Hz, 2H), 7.53 (d, $J = 8.2$ Hz, 2H), 5.00 (d, $J = 3.1$ Hz, 1H), 4.81 (s, 2H), 4.05 (t, $J = 9.7$ Hz, 1H), 3.61–3.44 (m, 1H), 1.64 (dtd, $J = 86.9, 11.2, 9.3, 4.9$ Hz, 6H).

General procedure for the synthesis of intermediates 17a–f. A solution of **11** (0.70 mmol), DIPEA (2.1 mmol), EDCI (1.82 mmol), HOBt (0.91 mmol) and the corresponding acids **14** (0.84 mmol) in DMF (5 ml) was stirred at room temperature for 5 h. The reaction was monitored by TLC. Upon completion, the mixture was diluted in H_2O (50 ml) and was extracted with EA (3×50 ml). The organic layer was separated, washed with water and brine, dried over Na_2SO_4. The drying agent was filtered off. The filtrate was concentrated under reduced pressure, and the residue was purified via column chromatography (DCM/MeOH $99:1\sim9:1$, v/v) to give the products as a light yellow liquid.

General procedure for the synthesis of the target compounds 18a–f. To a solution of **17** (0.45 mmol) in MeOH (3 ml) was added $TsOH\cdot H_2O$ (0.90 mmol) and stirred at room temperature for 8 h. The reaction was monitored by TLC. Upon completion, the mixture was concentrated *in vacuo*. Then, the residue was diluted in H_2O (10 ml) and was extracted with DCM (3×15 ml). The organic layer was separated, washed with saturated $NaHCO_3$ solution and brine, dried over Na_2SO_4. The drying agent was filtered off. The filtrate was concentrated under reduced pressure, and the residue was purified via C18 column chromatography (MeCN/H_2O $1:4\sim4:1$, v/v) to afford the products.

N^1-hydroxy-N^6-(2-((1R,3S,4S)-4-methyl-3-(prop-1-en-2-yl)-4-vinylcyclo-hexyl)allyl)adipamide (18a). White solid, yield 63.1%, m.p. 95.6–96.7 $^{\circ}C$. ^{1}H NMR (500 MHz, CDCl$_3$) δ 6.78 (t, $J = 5.9$ Hz, 1H), 5.80 (dd, $J = 17.7, 10.5$ Hz, 1H), 4.97–4.84 (m, 4H), 4.81 (s, 1H), 4.57 (s, 1H), 3.82 (d, $J = 5.6$ Hz, 2H), 2.22 (d, $J = 40.7$ Hz, 4H), 2.04–1.89 (m, 2H), 1.69 (s, 3H), 1.68–1.52 (m, 7H), 1.52–1.39 (m, 3H), 0.99 (s, 3H). ^{13}C NMR (126 MHz, CDCl$_3$) δ 173.76, 171.43, 150.40, 150.00, 147.41, 112.29, 110.07, 108.18, 52.65, 42.99, 42.69, 39.87, 39.77, 35.87, 33.08, 32.33, 27.21, 24.97, 24.92, 24.87, 16.61. HRMS (ESI) *m/z*: calcd for $C_{21}H_{34}N_2O_3$ $[M+H]^+$, 363.2642; found, 363.2641.

N^1-hydroxy-N^7-(2-((1R,3S,4S)-4-methyl-3-(prop-1-en-2-yl)-4-vinylcyclo-hexyl)allyl)heptanediamide (18b). Colourless viscous colloid, yield 58.9%, m.p. 55.7–58.1 $^{\circ}C$. ^{1}H NMR (500 MHz, CDCl$_3$) δ 6.35 (s, 1H), 5.80 (dd, $J = 17.7, 10.5$ Hz, 1H), 4.95–4.87 (m, 3H), 4.86 (s, 1H), 4.82 (t, $J = 1.7$ Hz, 1H), 4.57 (d, $J = 1.9$ Hz, 1H), 3.85 (d, $J = 5.6$ Hz, 2H), 2.29–2.11 (m, 4H), 2.04–1.90 (m, 2H), 1.70 (s, 3H), 1.68–1.53 (m, 5H), 1.52–1.40 (m, 3H), 1.40–1.24 (m, 4H), 0.99 (s, 3H). ^{13}C NMR (126 MHz, CDCl$_3$) δ 173.67, 171.44, 150.52, 149.99, 147.40, 112.27, 110.06, 108.32, 52.67, 43.00, 42.72, 39.85, 39.77, 36.16, 33.11, 32.36, 28.32, 27.20, 25.08, 24.89, 24.84, 16.61. HRMS (ESI) *m/z*: calcd for $C_{22}H_{36}N_2O_3$ $[M+H]^+$, 377.2799; found, 377.2798.

N^1-hydroxy-N^8-(2-((1R,3S,4S)-4-methyl-3-(prop-1-en-2-yl)-4-vinylcyclo-hexyl)allyl)octanediamide (18c). Colourless viscous colloid, yield 72.3%, m.p. 58.6–59.3 $^{\circ}C$. ^{1}H NMR (500 MHz, CDCl$_3$) δ 6.04 (s, 1H), 5.80 (dd, $J = 17.8, 10.5$ Hz, 1H), 4.96–4.76 (m, 5H), 4.58 (s, 1H), 3.86 (s, 2H), 2.27–2.09 (m, 4H), 2.02–1.91 (m, 2H), 1.70 (s, 3H), 1.64–1.30 (m, 14H), 1.00 (s, 3H). ^{13}C NMR (126 MHz, CDCl$_3$) δ 173.77, 171.50, 150.55, 150.00, 147.37, 112.28, 110.05, 108.30, 52.68, 42.98, 42.70, 39.86, 39.76, 36.37, 33.10, 29.69, 28.61, 28.40, 27.20, 25.53, 25.17, 24.84. HRMS (ESI) *m/z*: calcd for $C_{23}H_{38}N_2O_3$ $[M+H]^+$, 391.2955; found, 391.2955.

N-hydroxy-6–(4-(2-((1R,3S,4S)-4-methyl-3-(prop-1-en-2-yl)-4-vinylcyclo-hexyl)allyl)piperazin-1-yl)-6-oxohexanamide (18d). Colourless liquid, yield 70.3%. ^{1}H NMR (500 MHz, CDCl$_3$) δ 8.29 (s, 1H), 5.80 (dd, $J = 17.8, 10.5$ Hz, 1H), 5.12 (d, $J = 10.0$ Hz, 2H), 4.96–4.86 (m, 2H), 4.82 (s, 1H), 4.57 (s, 1H), 3.68 (d, $J = 46.1$ Hz, 4H), 3.28 (d, $J = 15.4$ Hz, 2H), 2.76 (d, $J = 40.0$ Hz, 4H), 2.36 (t, $J = 6.6$ Hz, 2H), 2.20 (t, $J = 5.9$ Hz, 2H), 2.04 (ddd, $J = 37.4, 12.2, 6.2$ Hz, 2H), 1.70 (s, 3H), 1.69–1.35 (m, 10H), 0.99 (s, 3H). ^{13}C NMR (126 MHz, CDCl$_3$) δ 171.96, 166.12, 149.99, 147.48, 147.05, 115.06, 112.21, 110.07, 62.15, 52.58 (d, $J = 18.0$ Hz), 52.05, 44.13, 41.63, 40.26, 39.76 (d, $J = 2.0$ Hz), 33.08, 32.38, 29.69, 27.14, 24.82 (d, $J = 11.0$ Hz), 24.19, 16.55. HRMS (ESI) *m/z*: calcd for $C_{25}H_{41}N_3O_3$ $[M+H]^+$, 432.3221; found, 432.3222.

N-hydroxy-7–(4-(2-((1R,3S,4S)-4-methyl-3-(prop-1-en-2-yl)-4-vinylcyclo-hexyl)allyl)piperazin-1-yl)-7-oxoheptanamide (18e). White solid, yield 60.7%, m.p. 126.7–127.5 $^{\circ}C$. ^{1}H NMR (500 MHz, DMSO-d_6) δ 10.32 (s, 1H), 8.65 (s, 1H), 5.82 (dd, $J = 17.9, 10.5$ Hz, 1H), 4.98–4.83 (m, 4H), 4.78 (p, $J = 1.5$ Hz, 1H), 4.58 (d, $J = 2.2$ Hz, 1H), 3.41 (q, $J = 5.8, 5.3$ Hz, 4H), 2.90 (q, $J = 13.4$ Hz, 2H), 2.33–2.22 (m, 6H), 2.11–1.99 (m, 2H), 1.93 (t, $J = 7.4$ Hz, 2H), 1.67 (s, 3H), 1.65–1.55 (m, 2H), 1.53–1.32 (m, 8H), 1.29–1.20 (m, 2H), 0.97 (s, 3H). ^{13}C NMR (126 MHz, DMSO-d_6) δ 170.93, 169.50, 150.83, 150.52, 147.63, 112.69, 111.53, 110.44, 63.18, 53.56, 53.07, 52.38, 45.46, 42.06, 41.52, 33.17, 32.63, 28.84, 27.21, 25.45, 25.01 (d, $J = 5.3$ Hz), 16.75. HRMS (ESI) *m/z*: calcd for $C_{26}H_{43}N_3O_3$ $[M+H]^+$, 446.3377; found, 446.3378.

N-hydroxy-8–(4-(2-((1R,3S,4S)-4-methyl-3-(prop-1-en-2-yl)-4-vinylcyclo-hexyl)allyl)piperazin-1-yl)-8-oxooctanamide (18f). White solid, yield 73.2%, m.p. 144.3–144.9 $^{\circ}C$. ^{1}H NMR (500 MHz, DMSO-d_6) δ 10.32 (s, 1H), 8.65 (s, 1H), 5.82 (dd, $J = 17.9, 10.5$ Hz, 1H), 4.96–4.82 (m, 4H), 4.78 (p, $J = 1.5$ Hz, 1H), 4.58 (d, $J = 2.3$ Hz, 1H), 3.41 (q, $J = 5.8$ Hz, 4H), 2.90 (q, $J = 13.4$ Hz, 2H), 2.34–2.19 (m, 6H), 2.11–1.98 (m, 2H), 1.93 (t, $J = 7.4$ Hz, 2H), 1.67 (s, 3H), 1.65–1.54 (m, 2H), 1.52–1.31 (m, 8H), 1.30–1.18 (m, $J = 4.8, 4.0$ Hz, 4H), 0.97 (s, 3H). ^{13}C NMR (126 MHz, DMSO-d_6) δ 170.98, 169.56, 150.82, 150.53, 147.63, 112.69, 111.54, 110.45, 63.18, 53.58, 53.08, 52.38, 45.48, 42.06, 41.52, 33.17, 32.70, 28.93 (d, $J = 6.7$ Hz), 27.21, 25.50, 25.18, 25.03, 16.75. HRMS (ESI) *m/z*: calcd for $C_{27}H_{45}N_3O_3$ $[M+H]^+$, 460.3534; found, 460.3538.

Synthesis of the intermediate 19. A solution of **11b** (0.52 mmol), DIPEA (0.78 mmol) and the benzyl chloride **16** (0.62 mmol) in DMF (4 ml) was stirred at $60\,^{\circ}C$ for 6 h. The reaction was monitored by TLC. Upon completion, the mixture was diluted in H_2O (40 ml) and was extracted with EA (3×30 ml). The organic layer was separated, washed with water and brine, dried over Na_2SO_4. The drying agent was filtered off. The filtrate was concentrated under reduced pressure and the residue was purified via flash column chromatography (DCM/MeOH 49:1, v/v) to give **19** (203.48 mg,

yield 75.0%) as a colourless liquid. ^{1}H NMR (400 MHz, CDCl$_3$) δ 8.75 (s, 1H), 7.63 (d, $J = 7.9$ Hz, 2H), 7.33 (d, $J = 7.9$ Hz, 2H), 5.75 (dd, $J = 17.6$, 10.7 Hz, 1H), 5.01 (s, 1H), 4.89–4.79 (m, 4H), 4.75 (t, $J = 1.8$ Hz, 1H), 4.54–4.48 (m, 1H), 3.99–3.89 (m, 1H), 3.64–3.55 (m, 1H), 3.47 (s, 2H), 2.91–2.79 (m, 2H), 2.37 (s, 8H), 1.98 (ddd, $J = 20.6$, 11.6, 4.3 Hz, 2H), 1.90–1.75 (m, 3H), 1.71–1.32 (m, 12H), 0.93 (s, 3H).

Synthesis of the target compound 20. To a solution of **19** (0.38 mmol) in MeOH (3 ml) was added TsOH·H$_2$O (0.76 mmol) and stirred at room temperature for 8 h. The reaction was monitored by TLC. Upon completion, the mixture was concentrated *in vacuo*. Then, the residue was diluted in H$_2$O (15 ml) and was extracted with DCM (3 × 15 ml). The organic layer was separated, washed with saturated NaHCO$_3$ solution and brine, dried over Na$_2$SO$_4$, and concentrated *in vacuo*. The residue was purified *via* C18 column chromatography (MeCN/H$_2$O 3:2, v/v) to afford **20** (141.35 mg, yield 85.1%) as a white solid, m.p. 99.4–100.2 °C. ^{1}H NMR (500 MHz, DMSO-d$_6$) δ 7.70 (d, $J = 8.3$ Hz, 2H), 7.35 (d, $J = 8.3$ Hz, 2H), 5.82 (dd, $J = 17.9$, 10.5 Hz, 1H), 4.91–4.84 (m, 4H), 4.77 (t, $J = 1.8$ Hz, 1H), 4.57 (d, $J = 2.2$ Hz, 1H), 3.32 (d, $J = 10.9$ Hz, 2H), 2.88 (q, $J = 13.3$ Hz, 2H), 2.36 (s, 8H), 2.08–1.95 (m, 2H), 1.66 (s, 3H), 1.64–1.51 (m, 2H), 1.50–1.39 (m, 3H), 1.36–1.31 (m, 1H), 0.96 (s, 3H). ^{13}C NMR (126 MHz, DMSO-d$_6$) δ 151.13, 150.53, 147.65, 142.07, 131.86, 129.10, 127.23, 112.65, 111.33, 110.42, 63.41, 62.10, 53.24 (d, $J = 7.1$ Hz), 52.40, 42.20, 33.18, 27.17, 25.02, 16.75. HRMS (ESI) *m/z*: calcd for C$_{27}$H$_{39}$N$_3$O$_2$ [M + H]$^+$, 438.3115; found, 438.3117.

Synthesis of the crucial intermediate 21. To a solution of β-elemene (**1**, 29.36 mmol) and tetrabutylammonium fluoride (TBAF, 1.0 mol/l THF) in DCM and AcOH was stirred at 0 °C. Then, NaClO solution (available chlorine $\geq$ 5.2%) was slowly added dropwise with a micro-injection pump within 5 h at 0 °C. The reaction was monitored by TLC. Upon completion, the reaction solution was slowly added to the saturated NaHCO$_3$ solution (until no bubbles were formed) at 0 °C. Then the mixture was extracted three times with PE (3 × 150 ml). The organic layer was separated, washed with brine, dried over Na$_2$SO$_4$, and concentrated *in vacuo*. The residue was purified *via* column chromatography (PE) to afford **21** (2.50 g, yield 31.17%) as a colourless liquid. ^{1}H NMR (400 MHz, CDCl$_3$) δ 5.79 (dd, $J = 17.2$, 11.1 Hz, 1H), 5.28 (s, 1H), 5.18 (s, 1H), 5.04 (s, 1H), 4.99–4.89 (m, 3H), 4.13–4.08 (m, 4H), 3.98 (d, $J = 11.7$ Hz, 1H), 3.78–3.66 (m, 2H), 2.36–2.21 (m, 2H), 1.78–1.40 (m, 10H), 0.99 (s, 3H).

Synthesis of intermediate 22a. To a solution of 13,14-Cl-β-elemene (**21**, 3.66 mmol) in DMF (10 ml) was added Cs$_2$CO$_3$ (4.39 mmol) and bis(tert-butoxycarbonyl)amine (4.39 mmol) successively at room temperature. Then mixture was stirred at 50 °C for 8 h. The reaction was monitored by TLC. Upon completion, the mixture was diluted in H$_2$O (100 ml) and was extracted with EA (3 × 100 ml). The combined organic layers were washed with water and brine, and dried over Na$_2$SO$_4$. The drying agent was filtered off. The filtrate was concentrated under reduced pressure and the residue was purified *via* flash column chromatography (PE/EA 1:4, v/v) to give **22a** (1244.71 mg, yield 74.9%) as a light yellow liquid. ^{1}H NMR (400 MHz, CDCl$_3$) δ 5.83–5.73 (m, 1H), 5.26 (d, $J = 1.0$ Hz, 1H), 4.98–4.86 (m, 4H), 4.77 (s, 1H), 4.20 (d, $J = 1.7$ Hz, 2H), 3.96 (dd, $J = 11.6$, 0.8 Hz, 1H), 2.98–2.87 (m, 1H), 2.31–2.20 (m, 1H), 2.00 (dd, $J = 11.1$, 4.0 Hz, 1H), 1.74–1.61 (m, 3H), 1.59–1.50 (m, 2H), 1.48 (s, 18H), 1.46–1.41 (m, 1H), 0.98 (s, 3H).

Synthesis of intermediate 22b. To a solution of 13,14-Cl-β-elemene (**21**, 1.77 mmol) in DMF (10 ml) was added Cs$_2$CO$_3$ (2.12 mmol) and 1-Boc-piperazine (2.12 mmol) successively at room temperature. Then mixture was stirred at 50 °C for 8 h. The reaction was monitored by TLC. Upon completion, the mixture was diluted in H$_2$O (100 ml) and was extracted with EA (3 × 100 ml). The combined organic layers were washed with water and brine, and dried over Na$_2$SO$_4$. The drying agent was filtered off. The filtrate was concentrated under reduced pressure and the residue was purified *via* flash column chromatography (PE/EA 1:3, v/v) to give **22b** (558.51 mg, yield 81.2%) as a light yellow liquid. ^{1}H NMR (400 MHz, CDCl$_3$) δ 5.79 (dd, $J = 17.4$, 10.8 Hz, 1H), 5.27 (s, 1H), 4.97–4.86 (m, 5H), 4.10 (dd, $J = 11.6$, 1.1 Hz, 1H), 3.97 (d, $J = 11.7$ Hz, 1H), 3.41 (t, $J = 4.9$ Hz, 4H), 2.98–2.86 (m, 2H), 2.32 (q, $J = 4.4$, 3.8 Hz, 4H), 2.30–2.25 (m, 1H), 2.14 (ddd, $J = 11.6$, 8.9, 6.1 Hz, 1H), 1.69–1.57 (m, 3H), 1.57–1.47 (m, 3H), 1.46 (s, 9H), 0.98 (s, 3H). LCMS *m/z* [M + H]$^+$: 423.5.

Synthesis of intermediate 24a. To a solution of **22a** (2.70 mmol) in DMF (10 ml) was added Cs$_2$CO$_3$ (4.05 mmol) and 1*H*-pyrazole (**23**, 3.24 mmol) successively at room temperature. Then mixture was stirred at 60 °C for 10 h. The reaction was monitored by TLC. Upon completion, the mixture was diluted in H$_2$O (100 ml) and was extracted with EA (3 × 100 ml). The combined organic layers were washed with water and brine, and dried over Na$_2$SO$_4$. The drying agent was filtered off. The filtrate was concentrated under reduced pressure and the residue was purified *via* flash column chromatography (PE/EA 3:1, v/v) to give **24a** (993.97 mg, yield 75.8%) as a light yellow liquid. ^{1}H NMR (400 MHz, CDCl$_3$) δ 7.50 (d, $J = 1.8$ Hz, 1H), 7.31 (d, $J = 2.3$ Hz, 1H), 6.25 (t, $J = 2.1$ Hz, 1H), 5.83 (dd, $J = 17.4$, 10.8 Hz, 1H), 5.05–4.96 (m, 2H), 4.85 (d, $J = 14.9$ Hz, 2H), 4.78 (s, 1H), 4.73 (dd, $J = 8.8$, 7.0 Hz, 2H), 4.65 (d, $J = 15.6$ Hz, 1H), 4.13 (d, $J = 1.9$ Hz, 2H), 1.94–1.80 (m, 2H), 1.72–1.49 (m, 6H), 1.47 (s, 18H), 1.02 (s, 3H).

Synthesis of intermediate 24b. To a solution of **22b** (2.22 mmol) in DMF (10 ml) was added Cs$_2$CO$_3$ (3.33 mmol) and 1*H*-pyrazole (**23**, 2.66 mmol) successively at room temperature. Then mixture was stirred at 60 °C for 10 h. The reaction was monitored by TLC. Upon completion, the mixture was diluted in H$_2$O (100 ml) and was extracted with EA (3 × 100 ml). The combined organic layers were washed with water and brine, and dried over Na$_2$SO$_4$. The drying agent was filtered off. The filtrate was concentrated under reduced pressure and the residue was purified *via* flash column chromatography (PE/EA 3:1, v/v) to give **24b** (789.31 mg, yield 78.2%) as a light yellow liquid. ^{1}H NMR (500 MHz, CDCl$_3$) δ 7.50 (d, $J = 1.9$ Hz, 1H), 7.33 (d, $J = 2.2$ Hz, 1H), 6.25 (t, $J = 2.1$ Hz, 1H), 5.84 (dd, $J = 17.4$, 10.8 Hz, 1H), 5.04–4.96 (m, 2H), 4.95–4.88 (m, 2H), 4.87 (s, 1H), 4.78 (s, 1H), 4.71 (d, $J = 1.4$ Hz, 1H), 4.66 (d, $J = 15.7$ Hz, 1H), 3.39 (s, 4H), 2.88 (q, $J = 13.5$ Hz, 2H), 2.36–2.25 (m, 4H), 2.00 (m, 1H), 1.93 (dd, $J = 12.7$, 3.4 Hz, 1H), 1.60–1.48 (m, 3H), 1.47 − 1.36 (m, 13H), 1.03 (s, 3H). LCMS *m/z* [M + H]$^+$: 455.5.

General procedure for the synthesis of intermediates 25a–b. To a solution of **24** (1.74 mmol) in MeOH (1.5 ml) in an ice-cooled bath was added a solution of hydrochloride in dioxane (4 M, 6 ml). The mixture was gradually warmed to room temperature and stirred for 8 h. The reaction was monitored by TLC. Upon completion, the solvent was removed under reduced pressure to give the intermediates **25** (1.74 mmol, yield 100%) as a white solid. The residue was used for the next reaction without further purification.

General procedure for the synthesis of intermediates 26a–f. A solution of **25** (0.52 mmol), DIPEA (1.56 mmol), EDCI (1.35 mmol), HOBt (0.68 mmol) and the corresponding acids (**14**, 0.62 mmol) in DMF (5 ml) was stirred at room temperature for 5 h. The reaction was monitored by TLC. Upon completion, the mixture was diluted in H_2O (50 ml) and was extracted with EA (3 × 50 ml). The organic layer was separated, washed with water and brine, dried over Na_2SO_4. The drying agent was filtered off. The filtrate was concentrated under reduced pressure, and the residue was purified *via* column chromatography (DCM/MeOH 99:1 ∼ 9:1, v/v) to give the products as a light yellow liquid.

General procedure for the synthesis of the target compounds 27a–f. To a solution of **26** (0.41 mmol) in MeOH (3 ml) was added TsOH·H_2O (0.82 mmol) and stirred at room temperature for 8 h. The reaction was monitored by TLC. Upon completion, the mixture was concentrated *in vacuo*. Then, the residue was diluted in H_2O (10 ml) and was extracted with DCM (3 × 10 ml). The organic layer was separated, washed with saturated $NaHCO_3$ solution and brine, dried over Na_2SO_4. The drying agent was filtered off. The filtrate was concentrated under reduced pressure, and the residue was purified *via* C18 column chromatography (MeCN/H_2O 1:4 ∼ 4:1, v/v) to afford the products.

N^1-(2-((1R,3R,4S)-3–(3-(1H-pyrazol-1-yl)prop-1-en-2-yl)-4-methyl-4-vinylcyclohexyl)allyl)-N^6-hydroxyadipamide (27a). White solid, yield 50.6%, m.p. 65.6–66.8 °C. ^{1}H NMR (500 MHz, CDCl$_3$) δ 7.48 (d, J = 1.8 Hz, 1H), 7.33 (d, J = 2.3 Hz, 1H), 6.25 (t, J = 2.1 Hz, 1H), 5.80 (dd, J = 17.4, 10.8 Hz, 1H), 5.04–4.95 (m, 2H), 4.84 (t, J = 5.9 Hz, 3H), 4.67 (d, J = 5.0 Hz, 3H), 3.79 (d, J = 5.3 Hz, 2H), 2.19 (d, J = 40.0 Hz, 4H), 1.96–1.80 (m, 2H), 1.73–1.36 (m, 10H), 1.00 (s, 3H). ^{13}C NMR (126 MHz, CDCl$_3$) δ 173.54, 150.18, 149.34, 147.43, 139.13, 129.85, 113.93, 111.41, 108.73, 105.73, 58.73, 48.08, 42.99, 42.30, 39.81, 39.65, 35.87, 33.33, 26.88, 25.02 (d, J = 7.6 Hz), 15.81. HRMS (ESI) m/z: calcd for C$_{24}$H$_{36}$N$_4$O$_3$ [M + H]$^+$, 429.2860; found, 429.2858.

N^1-(2-((1R,3R,4S)-3–(3-(1H-pyrazol-1-yl)prop-1-en-2-yl)-4-methyl-4-vinylcyclohexyl)allyl)-N^7-hydroxyheptanediamide (27b). Colourless viscous colloid, yield 42.8%, m.p. 47.3–49.0 °C. ^{1}H NMR (500 MHz, CDCl$_3$) δ 7.48 (s, 1H), 7.33 (d, J = 2.3 Hz, 1H), 6.25 (t, J = 2.0 Hz, 1H), 5.80 (dd, J = 17.4, 10.8 Hz, 1H), 5.10–4.94 (m, 2H), 4.85 (t, J = 4.1 Hz, 3H), 4.78–4.61 (m, 3H), 3.80 (s, 2H), 2.32–2.06 (m, 4H), 1.97–1.81 (m, 2H), 1.76–1.18 (m, 12H), 1.01 (s, 3H). ^{13}C NMR (126 MHz, CDCl$_3$) δ 173.52, 150.27, 149.31, 147.39, 139.14, 129.76, 114.13, 111.43, 108.78, 105.74, 58.81, 48.07, 42.94, 42.38, 39.82, 39.65, 36.12, 33.32, 29.70, 26.90, 25.07 (d, J = 23.7 Hz), 15.82. HRMS (ESI) m/z: calcd for C$_{25}$H$_{38}$N$_4$O$_3$ [M + H]$^+$, 443.3017; found, 443.3021.

N^1-(2-((1R,3R,4S)-3–(3-(1H-pyrazol-1-yl)prop-1-en-2-yl)-4-methyl-4-vinylcyclohexyl)allyl)-N^8-hydroxyoctanediamide (27c). Light yellow solid, yield 53.5%, m.p. 54.7–55.9 °C. ^{1}H NMR (500 MHz, CDCl$_3$) δ 7.48 (d, J = 2.0 Hz, 1H), 7.33 (d, J = 1.8 Hz, 1H), 6.25 (t, J = 2.1 Hz, 1H), 5.80 (dd, J = 17.4, 10.8 Hz, 1H), 5.04–4.95 (m, 2H), 4.85 (d, J = 5.9 Hz, 3H), 4.67 (dd, J = 28.0, 15.6 Hz, 3H), 3.81 (s, 2H), 2.28–2.03 (m, 4H), 1.95–1.81 (m, 2H), 1.72–1.16 (m, 14H), 1.01 (s, 3H). ^{13}C NMR (126 MHz, CDCl$_3$) δ 173.64, 150.26, 149.30, 147.36, 139.10, 129.71, 114.20, 111.44, 108.63, 105.74, 58.82, 48.04, 42.91, 42.35, 39.81, 39.65, 36.29, 33.31, 29.69, 28.55 (d, J = 17.1 Hz), 26.89, 25.52, 25.27, 15.81. HRMS (ESI) m/z: calcd for C$_{26}$H$_{40}$N$_4$O$_3$ [M + H]$^+$, 457.3173; found, 457.3172.

6–(4-(2-((1R,3R,4S)–3–(3-(1H-pyrazol-1-yl)prop-1-en-2-yl)-4-methyl-4-vinylcyclohexyl)allyl)piperazin-1-yl)-N-hydroxy-6-oxohexanamide (27d). Light yellow viscous colloid, yield 58.9%, m.p. 71.7–72.2 °C. ^{1}H NMR (500 MHz, CDCl$_3$) δ 7.50 (d, J = 1.8 Hz, 1H), 7.34 (d, J = 2.2 Hz, 1H), 6.25 (t, J = 2.1 Hz, 1H), 5.83 (dd, J = 17.4, 10.8 Hz, 1H), 5.10–4.83 (m, 5H), 4.81–4.62 (m, 3H), 3.57 (s, 2H), 3.43 (s, 2H), 2.89 (q, J = 13.4 Hz, 2H), 2.47–2.13 (m, 8H), 2.07–1.89 (m, 2H), 1.80–1.40 (m, 10H), 1.03 (s, 3H). ^{13}C NMR (126 MHz, CDCl$_3$) δ 171.66, 149.99, 149.46, 147.60, 139.12, 129.49, 114.20, 111.37 (d, J = 22.0 Hz), 105.60, 63.26, 59.01, 53.17, 52.81, 48.09, 45.64, 41.83 (d, J = 7.3 Hz), 39.90, 39.70, 33.66, 32.61, 29.69, 26.92, 24.89, 24.34, 15.82. HRMS (ESI) m/z: calcd for C$_{28}$H$_{43}$N$_5$O$_3$ [M + H]$^+$, 498.3439; found, 498.3436.

7–(4-(2-((1R,3R,4S)–3–(3-(1H-pyrazol-1-yl)prop-1-en-2-yl)-4-methyl-4-vinylcyclohexyl)allyl)piperazin-1-yl)-N-hydroxy-7-oxoheptanamide (27e). Colourless viscous colloid, yield 51.5%, m.p. 55.3–56.7 °C. ^{1}H NMR (500 MHz, CDCl$_3$) δ 7.50 (d, J = 1.9 Hz, 1H), 7.34 (d, J = 2.2 Hz, 1H), 6.25 (t, J = 2.1 Hz, 1H), 5.83 (dd, J = 17.4, 10.8 Hz, 1H), 5.07–4.84 (m, 5H), 4.80–4.63 (m, 3H), 3.65–3.36 (m, 4H), 2.90 (q, J = 13.4 Hz, 2H), 2.48–2.09 (m, 8H), 2.04–1.90 (m, 2H), 1.75–1.30 (m, 12H), 1.03 (s, 3H). ^{13}C NMR (126 MHz, CDCl$_3$) δ 171.78, 171.14, 149.97, 149.46, 147.59, 139.12, 129.51, 114.20, 111.49, 111.28, 105.60, 63.24, 59.02, 53.18, 52.81, 48.09, 45.67, 41.85, 39.90, 39.69, 33.67, 32.77, 32.33, 28.44, 26.90, 25.02, 24.47, 15.82. HRMS (ESI) m/z: calcd for C$_{29}$H$_{45}$N$_5$O$_3$ [M + H]$^+$, 512.3595; found, 512.3597.

7–(4-(2-((1R,3R,4S)–3–(3-(1H-pyrazol-1-yl)prop-1-en-2-yl)-4-methyl-4-vinylcyclohexyl)allyl)piperazin-1-yl)-N-hydroxy-7-oxoheptanamide (27f). Colourless viscous colloid, yield 68.7%, m.p. 59.6–60.0 °C. ^{1}H NMR (400 MHz, DMSO-d$_6$) δ 10.34 (s, 1H), 8.69 (s, 1H), 7.60 (d, J = 2.2 Hz, 1H), 7.42 (d, J = 1.8 Hz, 1H), 6.24 (t, J = 2.1 Hz, 1H), 5.87 (dd, J = 17.5, 10.8 Hz, 1H), 5.02–4.88 (m, 4H), 4.81 (s, 1H), 4.64 (s, 3H), 3.40 (d, J = 15.5 Hz, 4H), 2.86 (s, 2H), 2.24 (dt, J = 18.1, 6.1 Hz, 6H), 1.94 (dt, J = 14.7, 5.4 Hz, 4H), 1.68–1.32 (m, 10H), 1.32–1.17 (m, J = 4.7, 3.5 Hz, 4H), 0.99 (s, 3H). ^{13}C NMR (126 MHz, CDCl$_3$) δ 172.00, 171.16, 149.38, 148.88, 147.58, 139.09, 129.68, 113.97, 112.75, 111.32, 105.61, 62.90, 58.88, 53.10, 52.58, 48.12, 45.22, 41.69, 41.16, 39.85, 39.63, 33.60, 32.90, 32.60, 31.91, 30.30, 29.66 (d, J = 4.5 Hz), 28.50 (d, J = 20.2 Hz), 28.42, 26.83, 25.01 (d, J = 23.7 Hz), 15.82. HRMS (ESI) m/z: calcd for C$_{30}$H$_{47}$N$_5$O$_3$ [M + H]$^+$, 526.3752; found, 526.3755.

Synthesis of intermediate 28. (i) A solution of **25b** (1.00 mmol), DIPEA (3.00 mmol), EDCI (2.60 mmol), HOBt (1.30 mmol) and the acid **12c** (1.20 mmol) in DMF (6 ml) was stirred at room temperature for 5 h. The reaction was monitored by TLC. Upon completion, the mixture was diluted in H_2O (60 ml) and was extracted with EA (3 × 50 ml). The organic layer was separated, washed with water and brine, dried over Na_2SO_4. The drying agent was filtered off. The filtrate was concentrated under reduced pressure, and the residue was purified *via* column chromatography (DCM/MeOH 19:1, v/v) to give the ester (384.13 mg, yield 73.2%) as a light yellow liquid. ^{1}H NMR (500 MHz, CDCl$_3$) δ 7.43 (d, J = 2.0 Hz, 1H), 7.27 (d, J = 2.2 Hz, 1H), 6.18 (t, J = 2.1 Hz, 1H), 5.77 (dd, J = 17.5, 10.8 Hz, 1H), 5.02–4.78 (m, 5H), 4.66 (dd, J = 32.9, 17.4 Hz, 3H), 3.59 (s, 3H), 3.51 (s, 2H), 3.35 (s, 2H), 2.91–2.73 (m, 2H), 2.33–2.16 (m, 8H), 2.00–1.78 (m, 2H), 1.66–1.33 (m, 14H), 0.96 (s, 3H).

(ii) A solution of the ester (0.73 mmol) and cooled NaOH aqueous solution (1 N, 3 ml) in MeOH (3 ml) was stirred at room temperature for 2 h. The reaction was monitored by TLC. Upon completion, the mixture was concentrated in vacuo. Then, the

residue was neutralised by HCl solution (1 M) to pH 6 ∼ 7 and was extracted with EA (3 × 20 ml). The organic layer was separated, washed with water and brine, dried over Na_2SO_4. The drying agent was filtered off. The filtrate was concentrated under reduced pressure, and the resulted crude product (**28**, yield 90.6%) as a light yellow liquid, was directly used in the next reaction without purification.

Synthesis of the target compound 31. A solution of **28** (0.33 mmol), DIPEA (0.99 mmol), EDCI (0.86 mmol), HOBt (0.43 mmol) and *o*-phenylenediamine **29** (1.65 mmol) in DMF (6 ml) was stirred at room temperature for 5 h. The reaction was monitored by TLC. Upon completion, the mixture was diluted in H_2O (60 ml) and was extracted with EA (3 × 50 ml). The organic layer was separated, washed with water and brine, dried over Na_2SO_4. The drying agent was filtered off. The filtrate was concentrated under reduced pressure and the residue was purified *via* column chromatography (DCM/MeOH 19:1, v/v) to give the target compound **31** (90.61 mg, yield 45.7%) as a colourless viscous colloid, m.p. 59.7–60.5 °C. ^1H NMR (500 MHz, $CDCl_3$) δ 7.87 (s, 1H), 7.43 (d, J = 1.9 Hz, 1H), 7.26 (d, J = 2.3 Hz, 1H), 7.10 (dd, J = 7.8, 1.5 Hz, 1H), 6.95 (td, J = 7.6, 1.5 Hz, 1H), 6.73–6.64 (m, 2H), 6.18 (t, J = 2.1 Hz, 1H), 5.76 (dd, J = 17.5, 10.8 Hz, 1H), 5.00–4.77 (m, 5H), 4.73–4.54 (m, 3H), 3.50 (t, J = 5.0 Hz, 2H), 3.34 (t, J = 5.0 Hz, 2H), 2.89–2.73 (m, 2H), 2.37–2.13 (m, 8H), 2.00–1.80 (m, 2H), 1.68–1.27 (m, 14H), 0.96 (s, 3H). ^{13}C NMR (126 MHz, $CDCl_3$) δ 171.06, 170.57, 148.99, 148.45, 146.60, 139.84, 138.12, 128.40, 125.94, 124.26, 123.46, 118.25, 117.01, 113.23, 110.45, 110.26, 104.56, 62.23, 58.05, 52.22, 51.85, 47.06, 44.65, 40.87, 40.61, 38.88, 38.68, 35.63, 32.64, 32.04, 28.67, 27.77 (d, J = 13.2 Hz), 25.88, 24.55, 23.96, 14.79. HRMS (ESI) *m/z*: calcd for $C_{35}H_{50}N_6O_2$ $[M + H]^+$, 587.4068; found, 587.4066.

Synthesis of the target compound 32. A solution of **28** (0.31 mmol), DIPEA (0.93 mmol), EDCI (0.81 mmol), HOBt (0.40 mmol) and *o*-aminopyridine **30** (3.10 mmol) in DMF (5 ml) was stirred at room temperature for 5 h. The reaction was monitored by TLC. Upon completion, the mixture was diluted in H_2O (50 ml) and was extracted with EA (3 × 50 ml). The combined organic layers were washed with water and brine, and dried over Na_2SO_4. The drying agent was filtered off. The filtrate was concentrated under reduced pressure and the residue was purified *via* column chromatography (DCM/MeOH 97:3, v/v) to give the target compound **32** (91.14 mg, yield 50.1%) as a brown viscous colloid, m.p. 62.3–63.7 °C. ^1H NMR (500 MHz, $CDCl_3$) δ 8.62 (s, 1H), 8.27–8.16 (m, 2H), 7.67 (ddd, J = 8.8, 7.4, 1.9 Hz, 1H), 7.47 (d, J = 1.9 Hz, 1H), 7.31 (d, J = 2.1 Hz, 1H), 7.00 (ddd, J = 7.4, 4.9, 1.0 Hz, 1H), 6.22 (t, J = 2.1 Hz, 1H), 5.81 (dd, J = 17.4, 10.8 Hz, 1H), 5.04–4.93 (m, 2H), 4.92–4.82 (m, 3H), 4.75 (s, 1H), 4.73–4.61 (m, 2H), 3.56 (t, J = 5.0 Hz, 2H), 3.39 (t, J = 5.0 Hz, 2H), 2.86 (q, J = 13.4 Hz, 2H), 2.40–2.24 (m, 8H), 2.03–1.88 (m, 2H), 1.73–1.55 (m, 6H), 1.49–1.33 (m, 8H), 1.00 (s, 3H). ^{13}C NMR (126 MHz, $CDCl_3$) δ 171.92, 171.47, 151.62, 150.07, 149.46, 147.59 (d, J = 4.8 Hz), 139.12, 138.43, 129.36, 119.59, 114.20 (d, J = 13.5 Hz), 111.31 (d, J = 15.2 Hz), 105.56, 63.28, 59.07, 53.26, 52.89, 48.05, 45.66, 41.87, 41.60, 39.89, 39.69, 37.51, 33.66, 33.14, 29.68, 29.10, 28.90, 26.89, 25.12 (d, J = 7.7 Hz), 15.80. HRMS (ESI) *m/z*: calcd for $C_{36}H_{52}N_6O_2$ $[M + H]^+$, 601.4225; found, 601.4227.

Synthesis of intermediate 33. A solution of intermediate **25b** (0.34 mmol), DIPEA (0.51 mmol) and the benzyl chloride **16** (0.41 mmol) in DMF (2.5 ml) was stirred at 60 °C for 6 h. The reaction was monitored by TLC. Upon completion, the mixture was diluted in H_2O (25 ml) and was extracted with EA (3 × 25 ml). The combined organic layers were washed with water and brine, and

dried over Na_2SO_4. The drying agent was filtered off. The filtrate was concentrated under reduced pressure and the residue was purified *via* flash column chromatography (DCM/MeOH 19:1, v/v) to give **33** (131.80 mg, yield 65.9%) as a light yellow liquid. ^1H NMR (400 MHz, $CDCl_3$) δ 9.00 (s, 1H), 7.71 (d, J = 7.9 Hz, 2H), 7.51 (d, J = 1.8 Hz, 1H), 7.39 (d, J = 7.9 Hz, 2H), 7.33 (d, J = 2.3 Hz, 1H), 6.25 (t, J = 2.1 Hz, 1H), 5.83 (dd, J = 17.4, 10.8 Hz, 1H), 5.08 (d, J = 3.7 Hz, 1H), 5.04–4.95 (m, 2H), 4.93–4.89 (m, 1H), 4.86 (d, J = 2.5 Hz, 2H), 4.77–4.60 (m, 3H), 4.06–3.96 (m, 1H), 3.69–3.61 (m, 1H), 3.55 (s, 2H), 2.94–2.82 (m, 2H), 2.42 (s, 8H), 2.10–1.83 (m, 2H), 1.81–1.37 (m, 12H), 1.02 (s, 3H).

Synthesis of the target compound 34. To a solution of **33** (0.22 mmol) in MeOH (2 ml) was added $TsOH \cdot H_2O$ (0.44 mmol) and stirred at room temperature for 8 h. The reaction was monitored by TLC. Upon completion, the mixture was concentrated *in vacuo*. Then, the residue was diluted in H_2O (10 ml) and was extracted with DCM (3 × 10 ml). The organic layer was separated, washed with saturated $NaHCO_3$ solution and brine, dried over Na_2SO_4. The drying agent was filtered off. The filtrate was concentrated under reduced pressure and the residue was purified *via* C18 column chromatography (MeCN/H_2O 3:2, v/v) to afford the target compound **34** (74.58 mg, yield 67.3%) as a white solid, m.p. 111.8–112.6 °C. ^1H NMR (500 MHz, $CDCl_3$) δ 7.66 (d, J = 7.7 Hz, 2H), 7.48 (d, J = 1.6 Hz, 1H), 7.34–7.28 (m, 3H), 6.24 (t, J = 2.1 Hz, 1H), 5.79 (dd, J = 17.4, 10.8 Hz, 1H), 5.02–4.81 (m, 5H), 4.76–4.60 (m, 3H), 3.52 (s, 2H), 2.88 (q, J = 13.4 Hz, 2H), 2.46 (s, 8H), 2.04–1.87 (m, 2H), 1.63–1.36 (m, 6H), 1.00 (s, 3H). ^{13}C NMR (126 MHz, $CDCl_3$) δ 165.94, 150.16, 149.53, 147.65, 141.44, 139.12, 130.56, 129.55 (d, J = 5.5 Hz), 127.02, 113.98, 111.29 (d, J = 21.2 Hz), 105.62, 63.25, 62.44, 58.88, 52.85 (d, J = 16.7 Hz), 48.18, 41.95, 39.79 (d, J = 23.2 Hz), 33.64, 26.90, 15.81. HRMS (ESI) *m/z*: calcd for $C_{30}H_{41}N_5O_2$ $[M + H]^+$, 504.3333; found, 504.3333.

Synthesis of intermediate 35. To a solution of 13,14-Br-β-elemene (**21**, 4.93 mmol) in DMF (10 ml) was added Cs_2CO_3 (5.92 mmol) and 1*H*-pyrazole (**23**, 5.92 mmol) successively at room temperature. Then the mixture was stirred at 45 °C for 10 h. The reaction was monitored by TLC. Upon completion, the mixture was diluted in H_2O (100 ml) and was extracted with EA (3 × 100 ml). The combined organic layers were washed with water and brine, and dried over Na_2SO_4. The drying agent was filtered off. The filtrate was concentrated under reduced pressure and the residue was purified *via* flash column chromatography (PE/EA 4:1, v/v) to give **35** (1037.18 mg, yield 69.3%) as a light yellow liquid. ^1H NMR (500 MHz, $CDCl_3$) δ 7.53 (d, J = 1.6 Hz, 1H), 7.40 (d, J = 2.2 Hz, 1H), 6.28 (t, J = 2.1 Hz, 1H), 5.75 (dd, J = 17.3, 10.9 Hz, 1H), 5.26 (s, 1H), 5.02 (d, J = 1.2 Hz, 1H), 4.96–4.85 (m, 3H), 4.78 (s, 3H), 4.06 (dd, J = 11.7, 1.1 Hz, 1H), 3.95 (dd, J = 11.6, 0.8 Hz, 1H), 2.22 (dd, J = 12.5, 3.7 Hz, 1H), 1.95 (tt, J = 11.6, 3.7 Hz, 1H), 1.68–1.38 (m, 6H), 0.96 (s, 3H).

Synthesis of intermediate 36a. To a solution of intermediate **35** (2.89 mmol) in DMF (10 ml) was added Cs_2CO_3 (3.47 mmol) and bis(tert-butoxycarbonyl)amine (3.47 mmol) successively at room temperature. Then the mixture was stirred at 80 °C for 8 h. The reaction was monitored by TLC. Upon completion, the mixture was diluted in H_2O (100 ml) and was extracted with EA (3 × 100 ml). The combined organic layers were washed with water and brine, and dried over Na_2SO_4. The drying agent was filtered off. The filtrate was concentrated under reduced pressure and the residue was purified *via* flash column chromatography (PE/EA 7:3, v/v) to give **36a** (1056.24 mg, yield 75.5%) as a light yellow liquid.

^{1}H NMR (400 MHz, CDCl$_3$) δ 7.51 (d, J = 1.8 Hz, 1H), 7.39 (d, J = 2.2 Hz, 1H), 6.27 (t, J = 2.1 Hz, 1H), 5.85–5.76 (m, 1H), 5.01 (s, 1H), 4.94 (q, J = 1.3 Hz, 1H), 4.92–4.89 (m, 1H), 4.86 (d, J = 1.8 Hz, 1H), 4.74 (d, J = 7.0 Hz, 4H), 4.22 (dt, J = 17.0, 2.0 Hz, 1H), 3.89 (d, J = 17.0 Hz, 1H), 1.94–1.83 (m, 2H), 1.72–1.53 (m, 3H), 1.48 (s, 3H), 1.47 (s, 18H), 0.99 (s, 3H).

Synthesis of intermediate 36b.

To a solution of intermediate **35** (1.98 mmol) in DMF (7 ml) was added Cs$_2$CO$_3$ (2.38 mmol) and 1-Boc-piperazine (2.38 mmol) successively at room temperature. Then the mixture was stirred at 80 °C for 8 h. The reaction was monitored by TLC. Upon completion, the mixture was diluted in H$_2$O (70 ml) and was extracted with EA (3 × 70 ml). The combined organic layers were washed with water and brine, and dried over Na$_2$SO$_4$. The drying agent was filtered off. The filtrate was concentrated under reduced pressure and the residue was purified via flash column chromatography (PE/EA 3:1, v/v) to give **36b** (781.72 mg, yield 86.8%) as a light yellow liquid. ^{1}H NMR (400 MHz, CDCl$_3$) δ 7.55 (d, J = 1.8 Hz, 1H), 7.42 (d, J = 2.3 Hz, 1H), 6.31 (t, J = 2.1 Hz, 1H), 5.80 (dd, J = 17.5, 10.7 Hz, 1H), 5.06 (d, J = 8.0 Hz, 2H), 4.94–4.86 (m, 2H), 4.80 (d, J = 3.8 Hz, 4H), 3.43 (s, 4H), 3.06 (d, J = 13.8 Hz, 1H), 2.64 (d, J = 13.7 Hz, 1H), 2.42–2.31 (m, 2H), 2.22 (s, 2H), 1.91 (d, J = 11.1 Hz, 1H), 1.80 (s, 1H), 1.69–1.56 (m, 2H), 1.55–1.50 (m, 1H),1.50–1.425 (m, 12H), 1.00 (s, 3H). LCMS m/z [M + H]$^+$: 454.9.

General procedure for the synthesis of intermediates 37a–b.

To a solution of intermediate **36** (1.55 mmol) in MeOH (1.5 ml) in an ice-cooled bath was added a solution of hydrochloride in dioxane (4 M, 6 ml). The mixture was gradually warmed to room temperature and stirred for 8 h. The reaction was monitored by TLC. Upon completion, the solvent was removed under reduced pressure to give intermediates **37** (1.55 mmol, yield 100%) as a white solid. The residue was used for the next reaction without further purification.

General procedure for the synthesis of intermediates 38a–f.

A solution of **37** (0.41 mmol), DIPEA (1.23 mmol), EDCI (1.07 mmol), HOBt (0.53 mmol) and the corresponding acids **14** (0.49 mmol) in DMF (5 ml) was stirred at room temperature for 5 h. The reaction was monitored by TLC. Upon completion, the mixture was diluted in H$_2$O (50 ml) and was extracted with EA (3 × 50 ml). The combined organic layers were washed with water and brine, and dried over Na$_2$SO$_4$. The drying agent was filtered off. The filtrate was concentrated under reduced pressure and the residue was purified via column chromatography (DCM/MeOH 99:1 ~ 9:1, v/v) to give the products as a light yellow liquid.

General procedure for the synthesis of the target compounds 39a–f.

To a solution of intermediates **38** (0.37 mmol) in MeOH (3 ml) was added TsOH·H$_2$O (0.74 mmol) in room temperature for 8 h. The reaction was monitored by TLC. Upon completion, the mixture was concentrated in vacuo. Then, the mixture was diluted in H$_2$O (10 ml) and was extracted with DCM (3 × 10 ml). The combined organic layers were washed with water and brine, and dried over Na$_2$SO$_4$. The drying agent was filtered off. The filtrate was concentrated under reduced pressure and the residue was purified via C18 column chromatography (MeCN/H$_2$O 1:4 ~ 4:1, v/v) to afford the products.

N^1-(2-((1R,2S,5R)-5–(3-(1H-pyrazol-1-yl)prop-1-en-2-yl)-2-methyl-2-vinylcyclohexyl)allyl)-N^6-hydroxyadipamide (39a).

White solid, yield 70.4%, m.p. 61.7–63.3 °C. ^{1}H NMR (500 MHz, CDCl$_3$) δ 7.49 (s, 1H), 7.40 (d, J = 2.3 Hz, 1H), 6.28 (t, J = 2.1 Hz, 1H), 5.76 (dd, J = 17.4, 10.8 Hz, 1H), 5.08–4.62 (m, 8H), 3.83 (dd, J = 15.6, 6.4 Hz, 1H), 3.61 (dd, J = 15.8, 4.6 Hz, 1H), 2.19 (d, J = 28.1 Hz, 4H), 1.93 (d, J = 10.9 Hz, 1H), 1.83 (s, 1H), 1.72–1.38 (m, 10H), 0.96 (s, 3H). ^{13}C NMR (126 MHz, CDCl$_3$) δ 173.40, 149.46, 149.14, 147.90, 139.12, 129.66, 112.34, 111.63, 110.98, 106.00, 56.17, 48.97, 46.09, 41.57, 39.68, 39.41, 35.90, 33.45, 32.32, 26.76, 24.93 (d, J = 14.8 Hz), 16.04. HRMS (ESI) m/z: calcd for C$_{24}$H$_{36}$N$_4$O$_3$ [M + H]$^+$, 429.2860; found, 429.2863.

N^1-(2-((1R,2S,5R)-5–(3-(1H-pyrazol-1-yl)prop-1-en-2-yl)-2-methyl-2-vinylcyclohexyl)allyl)-N^7-hydroxyheptanediamide (39b).

Colourless viscous colloid, yield 72.5%, m.p. 63.8–64.9 °C. ^{1}H NMR (500 MHz, CDCl$_3$) δ 7.49 (s, 1H), 7.40 (d, J = 2.2 Hz, 1H), 6.27 (s, 1H), 5.76 (dd, J = 17.4, 10.8 Hz, 1H), 4.97 (d, J = 11.2 Hz, 2H), 4.89 (dd, J = 14.2, 10.5 Hz, 2H), 4.73 (q, J = 9.9, 8.5 Hz, 4H), 3.80 (d, J = 17.2 Hz, 1H), 3.63 (d, J = 13.7 Hz, 1H), 2.16 (d, J = 36.6 Hz, 4H), 1.98–1.79 (m, 2H), 1.72–1.37 (m, 8H), 1.36–1.20 (m, 4H), 0.96 (s, 3H). ^{13}C NMR (126 MHz, CDCl$_3$) δ 173.46, 149.47, 149.18, 147.95, 139.16, 129.61, 111.61, 110.95, 105.94, 56.11, 49.13, 45.89, 41.70, 39.67, 39.40, 36.11, 33.33, 29.70, 26.78, 16.12. HRMS (ESI) m/z: calcd for C$_{25}$H$_{38}$N$_4$O$_3$ [M + H]$^+$, 443.3017; found, 443.3014.

N^1-(2-((1R,2S,5R)-5–(3-(1H-pyrazol-1-yl)prop-1-en-2-yl)-2-methyl-2-vinylcyclohexyl)allyl)-N^8-hydroxyoctanediamide (39c).

White solid, yield 59.7%, m.p. 55.4–57.9 °C. ^{1}H NMR (500 MHz, CDCl$_3$) δ 10.16 (s, 1H), 7.43 (d, J = 1.9 Hz, 1H), 7.33 (d, J = 2.2 Hz, 1H), 6.21 (t, J = 2.1 Hz, 1H), 6.08 (s, 1H), 5.70 (dd, J = 17.4, 10.8 Hz, 1H), 4.97–4.79 (m, 4H), 4.75–4.62 (m, 4H), 3.78 (dd, J = 15.8, 6.5 Hz, 1H), 3.56 (dd, J = 15.8, 4.7 Hz, 1H), 2.09 (dt, J = 26.4, 7.4 Hz, 4H), 1.86 (dd, J = 12.5, 3.3 Hz, 1H), 1.82–1.72 (m, 1H), 1.59–1.34 (m, 10H), 1.24 (dd, J = 7.9, 4.0 Hz, 4H), 0.90 (s, 3H). ^{13}C NMR (126 MHz, CDCl$_3$) δ 173.42, 171.15, 149.42, 149.15, 148.02, 139.12, 129.57, 112.18, 111.68, 110.98, 105.97, 56.14, 49.09, 45.97, 41.63, 39.68, 39.46, 36.29, 33.41, 32.62, 28.42, 28.30, 26.74, 25.41, 25.12, 21.06, 16.03, 14.20. HRMS (ESI) m/z: calcd for C$_{26}$H$_{40}$N$_4$O$_3$ [M + H]$^+$, 457.3173; found, 457.3177.

6–(4-(2-((1R,2S,5R)-5–(3-(1H-pyrazol-1-yl)prop-1-en-2-yl)-2-methyl-2-vinylcyclohexyl)allyl)piperazin-1-yl)-N-hydroxy-6-oxohexanamide (39d).

Light yellow solid, yield 72.5%, m.p. 100.2–102.3 °C. ^{1}H NMR (500 MHz, CDCl$_3$) δ 7.50 (d, J = 1.9 Hz, 1H), 7.40 (d, J = 2.2 Hz, 1H), 6.27 (t, J = 2.1 Hz, 1H), 5.75 (dd, J = 17.5, 10.8 Hz, 1H), 5.02 (d, J = 11.3 Hz, 2H), 4.91–4.83 (m, 2H), 4.76 (d, J = 1.8 Hz, 4H), 3.58 (s, 2H), 3.50–3.34 (m, 2H), 3.02 (d, J = 13.8 Hz, 1H), 2.60 (d, J = 13.8 Hz, 1H), 2.43–2.12 (m, 9H), 1.90 (dt, J = 11.4, 6.9 Hz, 1H), 1.71–1.21 (m, 10H), 0.96 (s, 3H). ^{13}C NMR (126 MHz, CDCl$_3$) δ 171.75, 149.75, 149.70, 147.71, 139.16, 129.35, 114.09, 111.60, 110.42, 105.79, 66.01, 56.31, 53.09, 52.89, 47.77, 45.64, 41.90, 39.77 (d, J = 7.9 Hz), 36.50, 33.57, 32.68, 26.97, 25.28, 24.63, 15.86. HRMS (ESI) m/z: calcd for C$_{28}$H$_{43}$N$_5$O$_3$ [M + H]$^+$, 498.3439; found, 498.3440.

7–(4-(2-((1R,2S,5R)-5–(3-(1H-pyrazol-1-yl)prop-1-en-2-yl)-2-methyl-2-vinylcyclohexyl)allyl)piperazin-1-yl)-N-hydroxy-7-oxoheptanamide (39e).

Light yellow solid, yield 70.8%, m.p. 60.2–61.3 °C. ^{1}H NMR (500 MHz, CDCl$_3$) δ 7.43 (d, J = 1.9 Hz, 1H), 7.33 (d, J = 2.3 Hz, 1H), 6.21 (t, J = 2.1 Hz, 1H), 5.69 (dd, J = 17.5, 10.8 Hz, 1H), 4.96 (d, J = 10.5 Hz, 2H), 4.89–4.63 (m, 6H), 3.61–3.28 (m, 4H), 2.98 (d, J = 13.6 Hz, 1H), 2.55 (d, J = 13.7 Hz, 1H), 2.41–2.04 (m, 9H), 1.83 (ddt, J = 11.6, 8.2, 3.3 Hz, 1H), 1.66–1.23 (m, 12H), 0.90 (s, 3H). ^{13}C NMR (126 MHz, CDCl$_3$) δ 170.80, 170.08, 148.66 (d, J = 4.8 Hz),

146.59, 138.13, 128.37, 113.38, 110.70, 109.44, 104.83, 65.08, 55.36, 52.09, 51.79, 46.76, 44.67, 40.75 (d, $J = 9.0$ Hz), 38.74 (d, $J = 2.3$ Hz), 32.62, 31.76, 31.36, 27.41, 25.93, 23.98, 23.45, 14.81. HRMS (ESI) m/z: calcd for $C_{29}H_{45}N_5O_3$ [M + H]$^+$, 512.3595; found, 512.3596.

8–(4-(2-((1R,2S,5R)-5–(3-(1H-pyrazol-1-yl)prop-1-en-2-yl)-2-methyl-2-vinylcyclohexyl)allyl)piperazin-1-yl)-N-hydroxy-8-oxooctanamide (39f). Colourless viscous colloid, yield 60.3%, m.p. 58.7–59.5 °C. ^{1}H NMR (500 MHz, CDCl$_3$) δ 7.50 (d, $J = 1.8$ Hz, 1H), 7.40 (d, $J = 2.2$ Hz, 1H), 6.28 (t, $J = 2.1$ Hz, 1H), 5.76 (dd, $J = 17.5$, 10.7 Hz, 1H), 5.03 (d, $J = 10.4$ Hz, 2H), 4.95–4.83 (m, 2H), 4.83–4.68 (m, 4H), 3.58 (s, 2H), 3.45 (tdd, $J = 15.2$, 7.5, 4.0 Hz, 2H), 3.04 (d, $J = 13.6$ Hz, 1H), 2.61 (d, $J = 13.7$ Hz, 1H), 2.49–2.10 (m, 9H), 1.96–1.84 (m, 1H), 1.74–1.18 (m, 14H), 0.97 (s, 3H). ^{13}C NMR (126 MHz, CDCl$_3$) δ 171.89, 149.72, 149.68, 147.66, 139.15, 129.37, 114.31, 111.71, 110.44, 105.84, 66.12, 56.38, 53.19, 52.84, 47.78, 45.75, 41.82, 41.70, 39.76 (d, $J = 2.4$ Hz), 33.64, 32.95, 32.44, 32.42, 28.47 (d, $J = 18.9$ Hz), 26.96, 25.01 (d, $J = 17.6$ Hz), 15.84. HRMS (ESI) m/z: calcd for $C_{30}H_{47}N_5O_3$ [M + H]$^+$, 526.3752; found, 526.3752.

Synthesis of the compound 40. (i) A solution of **37a** (0.35 mmol), DIPEA (1.05 mmol), EDCI (0.91 mmol), HOBt (0.46 mmol) and the acid (**12c**, 0.42 mmol) in DMF (3 ml) was stirred at room temperature for 5 h. The reaction was monitored by TLC. Upon completion, the residue was diluted in H$_2$O (30 ml) and was extracted with EA (3 × 30 ml). The combined organic layers were washed with water and brine, and dried over Na$_2$SO$_4$. The drying agent was filtered off. The filtrate was concentrated under reduced pressure and the residue was purified via column chromatography (DCM/MeOH 49:1, v/v) to give the corresponding ester (153.00 mg, yield 95.7%) as a light yellow liquid.

(ii) A solution of the ester (0.28 mmol) and cooled NaOH aqueous solution (1 N, 3 ml) in MeOH (3 ml) was stirred at room temperature for 2 h. The reaction was monitored by TLC. Upon completion, the mixture was concentrated in vacuo. Then, the residue was neutralised by HCl solution (1 M) to pH 6∼7 and was extracted with EA (3 × 20 ml). The combined organic layers were washed with water and brine, and dried over Na$_2$SO$_4$. The drying agent was filtered off. The filtrate was concentrated under reduced pressure to afford the crude product **40** (yield 92.3%) as a light yellow liquid. It was directly used in the next reaction without purification.

Synthesis of the target compound 41. A solution of **40** (0.12 mmol), DIPEA (0.36 mmol), EDCI (0.31 mmol), HOBt (0.16 mmol) and o-phenylenediamine **29** (0.60 mmol) in DMF (3 ml) was stirred at room temperature for 5 h. The reaction was monitored by TLC. Upon completion, the mixture was diluted in H$_2$O (30 ml) and was extracted with EA (3 × 30 ml). The combined organic layers were washed with water and brine, and dried over Na$_2$SO$_4$. The drying agent was filtered off. The filtrate was concentrated under reduced pressure and the residue was purified via C18 column chromatography (MeCN/H$_2$O 2:3∼1:1, v/v) to afford **41** (56.11 mg, yield 88.0%) as a light yellow solid, m.p. 98.2–100.3 °C. ^{1}H NMR (500 MHz, CDCl$_3$) δ 7.83 (s, 1H), 7.51 (d, $J = 1.9$ Hz, 1H), 7.39 (d, $J = 2.2$ Hz, 1H), 7.16 (dd, $J = 7.7$, 1.4 Hz, 1H), 7.03 (td, $J = 7.7$, 1.5 Hz, 1H), 6.76 (t, $J = 7.6$ Hz, 2H), 6.28 (t, $J = 2.1$ Hz, 1H), 5.75 (dd, $J = 17.5$, 10.8 Hz, 1H), 4.99 (s, 1H), 4.97–4.86 (m, 3H), 4.79–4.69 (m, 4H), 3.84 (dd, $J = 15.8$, 6.8 Hz, 1H), 3.62 (dd, $J = 15.8$, 5.0 Hz, 1H), 2.37 (t, $J = 7.5$ Hz, 2H), 2.19 (t, $J = 7.4$ Hz, 2H), 1.94–1.80 (m, 2H), 1.77–1.49 (m, 5H), 1.48–1.24 (m, 9H), 0.96 (s, 3H). ^{13}C NMR (126 MHz, CDCl$_3$) δ 172.90, 172.03, 149.41, 149.15,

148.09, 140.83, 139.19, 129.42, 126.98, 125.24, 124.47, 119.31, 118.10, 112.11, 111.70, 110.98, 105.88, 56.18, 49.12, 45.89, 41.73, 39.69, 39.48, 36.65, 36.39, 33.38, 28.62, 28.23, 26.80, 25.51, 25.29, 15.98. HRMS (ESI) m/z: calcd for $C_{32}H_{45}N_5O_2$ [M + H]$^+$, 532.3646; found, 532.3647.

Synthesis of intermediate 42. A solution of **37b** (0.37 mmol), DIPEA (0.44 mmol) and the benzyl chloride **16** (0.44 mmol) in DMF (3 ml) was stirred at 60 °C for 6 h. The reaction was monitored by TLC. Upon completion, the mixture was diluted in H$_2$O (30 ml) and was extracted with EA (3 × 30 ml). The combined organic layers were washed with water and brine, and dried over Na$_2$SO$_4$. The drying agent was filtered off. The filtrate was concentrated under reduced pressure and the residue was purified via flash column chromatography (DCM/MeOH 91:9, v/v) to give **42** (196.39 mg, yield 90.3%) as a colourless liquid. ^{1}H NMR (500 MHz, CDCl$_3$) δ 7.76–7.67 (m, 2H), 7.49 (d, $J = 1.9$ Hz, 1H), 7.42–7.34 (m, 3H), 6.25 (t, $J = 2.1$ Hz, 1H), 5.74 (dd, $J = 17.5$, 10.8 Hz, 1H), 5.10–5.03 (m, 2H), 4.99 (s, 1H), 4.88–4.71 (m, 6H), 4.00 (td, $J = 10.4$, 9.1, 2.9 Hz, 1H), 3.63 (dd, $J = 10.4$, 4.9 Hz, 1H), 3.60 (s, 2H), 3.09 (d, $J = 13.5$ Hz, 1H), 2.68 (d, $J = 13.6$ Hz, 1H), 2.62–2.22 (m, 8H), 2.15 (dd, $J = 12.6$, 3.6 Hz, 1H), 1.96–1.76 (tdd, $J = 17.0$, 12.5, 9.5 Hz, 4H), 1.75–1.35 (m, 9H), 0.94 (s, 3H).

Synthesis of the target compound 43. To a solution of **42** (0.26 mmol) in MeOH (2 ml) was added TsOH·H$_2$O (0.52 mmol) and stirred at room temperature for 8 h. The reaction was monitored by TLC. Upon completion, the mixture was concentrated in vacuo. Then, the residue was diluted in H$_2$O (10 ml) and was extracted with DCM (3 × 10 ml). The organic layer was separated, washed with saturated NaHCO$_3$ solution and brine, and dried over Na$_2$SO$_4$. The drying agent was filtered off. The filtrate was concentrated under reduced pressure and the residue was purified via C18 column chromatography (MeCN/H$_2$O 1:1, v/v) to afford the target compound **43** (95.73 mg, yield 73.1%) as a white solid, m.p. 103.2–105.3 °C. ^{1}H NMR (500 MHz, CDCl$_3$) δ 7.65 (d, $J = 7.7$ Hz, 2H), 7.48 (d, $J = 1.9$ Hz, 1H), 7.38 (d, $J = 2.3$ Hz, 1H), 7.32 (d, $J = 7.7$ Hz, 2H), 6.25 (t, $J = 2.1$ Hz, 1H), 5.74 (dd, $J = 17.5$, 10.8 Hz, 1H), 5.00 (d, $J = 11.1$ Hz, 2H), 4.90–4.69 (m, 6H), 3.53 (s, 2H), 3.02 (d, $J = 13.6$ Hz, 1H), 2.61 (d, $J = 13.6$ Hz, 1H), 2.45 (s, 8H), 2.14 (dd, $J = 11.7$, 4.4 Hz, 1H), 1.89 (dq, $J = 11.8$, 4.4, 4.0 Hz, 1H), 1.64–1.35 (m, 6H), 0.94 (s, 3H). ^{13}C NMR (126 MHz, CDCl$_3$) δ 149.72 (d, $J = 4.0$ Hz), 147.70, 139.17, 129.50 (d, $J = 11.8$ Hz), 126.95, 114.32, 111.50, 110.35, 105.83, 66.20, 62.49, 56.34, 52.87 (d, $J = 14.0$ Hz), 47.94, 41.81, 39.69, 33.64, 26.90, 15.85. HRMS (ESI) m/z: calcd for $C_{30}H_{41}N_5O_2$ [M + H]$^+$, 504.3333; found, 504.3337.

Biological evaluation

HDAC inhibition assay

All HDAC enzymes were purchased from BPS Bioscience. The various concentrations of the tested compounds and HDAC isoforms were mixed into a 384-well plate and incubated at 37 °C for 10 min. Then the diluted HDAC substrate was added into each well and incubated at 37 °C for 30 min. The reaction was stopped by adding developer, and the mixture was incubated at 37 °C for another 20 min. The fluorescence intensity was measured at the excitation and emission wavelengths of 355 nm and 460 nm with a microplate reader. The IC$_{50}$ values were calculated according to the dose dependent curves. All the tests were repeated in three independent experiments.

In vitro anti-proliferative assay

The anti-proliferative activities of the target compounds were determined using CCK8 assay kit. 80 μL of cell suspensions (5.0×10^4 cell/ml) (K562, MV4-11, HEL, SU-DHL-2, WSU-DLCL-2 and U87MG) were added to a 96-well cell culture plate and incubated for 24 h at 37 °C under an atmosphere of 5% CO_2. The tested compounds were dissolved in the culture medium with 0.5% DMSO at the different concentrations. The cells were treated with the drug solution for another 72 h. Then 10 μL of cell counting kit-8 (CCK8) solution was added to each well and the plate was incubated for an additional 1 h. The IC_{50} values were calculated according to the dose dependent curves. All the tests were repeated in three independent experiments.

Apoptosis assay

WSU-DLCL-2 cells were seeded into 6-well plates and incubated at 37 °C for 24 h, and then treated with the tested compounds at the different concentrations or without the tested compound for another 72 h. The cells were then harvested by trypsinization and washed twice with cold PBS. After the centrifugation and removal of the supernatants, cells were re-suspended in 500 μL of a $1 \times$ binding buffer, which was then added to 5 μL of annexin V-FITC and 10 μL of PI, and incubated at room temperature for 15 min in the dark. The stained cells were analysed by a flow cytometer.

Cell cycle assay

WSU-DLCL-2 cells were seeded into 6-well plates and incubated at 37 °C for 24 h, and then treated with the tested compounds at the different concentrations or without the tested compound for another 72 h. After treatment, cells were collected and fixed with 70% pre-cold ethanol in PBS and stored at −20 °C overnight. Then washed the cells with PBS twice, and incubated with 100 μg/ml RNase A at 37 °C for 1 h, stained with propidium iodide for 30 min avoid light at room temperature. The stained cells were analysed by a flow cytometer.

Molecular docking

The molecular docking was performed using energetics (CDOCER) software (Discovery Studio® 2020). The two-dimensional structure of HDAC1 (PDB code: 5ICN) and HDAC6 (PDB code: 5EDU) was performed from the Protein Data Bank. The binding water and ligands were deleted and the polar hydrogen was added. The molecular structures of compounds **27f** and **39f** were optimised using Tripos force field. The molecular docking of **27f** and **39f** with HDAC1 and HDAC6 was carried out with Discovery Studio® 2020.

Pharmacokinetics study

The experimental procedures and the animal use and care protocols were approved by the Committee on Ethical Use of Animals of Hangzhou Normal University. Compound **27f** was subjected to PK studies in ICR (SPF) female mice. Compound **27f** was dissolved in the solution of 0.5% methylcellulose (containing 0.4% Tween 80) and then administrated via the oral route at 10 mg/kg (twelve rats). Compound **27f** was dissolved in the solution of 5% dimethyl sulfoxide (DMSO), 5% Solutol, and 90% saline and then administrated via the intravenous route at 5 mg/kg (twelve rats). At time points 0 (prior to dosing), 5, 15, 30, 60, 120, 240, 480, and 1440 min after dosing, the blood sample was collected from each animal, and the plasma was separated from the blood by centrifugation and stored in a freezer at −80 °C. All samples for the tested compound were analysed by liquid chromatography-tandem mass spectrometry (LC-MS/MS).

Disclosure statement

The authors report no conflicts of interest.

References

1.　Zhai B, Zhang N, Han X, et al. Molecular targets of β-elemene, a herbal extract used in traditional Chinese medicine, and its potential role in cancer therapy: a review. Biomed Pharmacother. 2019;114:108812.
2.　Xie T. Elemene antitumor drugs: molecular compatibility theory and its applications in new drug development and clinical practice. 1st ed. Amsterdam: Elsevier; 2022.
3.　Zheng F, Tang Q, Zheng X, et al. Inactivation of Stat3 and crosstalk of miRNA155-5p and FOXO3a contribute to the induction of IGFBP1 expression by beta-elemene in human lung cancer. Exp Mol Med. 2018;50:121.
4.　Long J, Liu Z, Hui L. Anti-tumor effect and mechanistic study of elemene on pancreatic carcinoma. BMC Complem Altern M. 2019;19:133.
5.　Xu L, Guo T, Qu X, et al. β-Elemene increases the sensitivity of gastric cancer cells to TRAIL by promoting the formation of DISC in lipid rafts. Cell Biol Int. 2018;42:1377.
6.　Xie L, Zhang J, Yan H, et al. β-Elemene induced apoptosis and senescence of triple-negative breast cancer cells through IGF1/IGF1R pathway. Tissue Cell. 2022;79:101914.
7.　Cai B, Ma L, Nong S, et al. β-Elemene induced anticancer effect in bladder cancer through upregulation of PTEN and suppression of AKT phosphorylation. Oncol Lett. 2018;16:6019.
8.　Li C-L, Chang L, Guo L, et al. β-Elemene induces caspasedependent apoptosis in human glioma cells in vitro through the upregulation of Bax and Fas/FasL and downregulation of Bcl-2. Asian Pac J Cancer Prev. 2014;15:10407.
9.　Wang G, Li X, Huang F, et al. Antitumor effect of beta-elemene in non-small-cell lung cancer cells is mediated via induction of cell cycle arrest and apoptotic cell death. Cell Mol Life Sci. 2005;62:881.
10.　Liu J, Zhang Y, Qu J, et al. β-Elemene-induced autophagy protects human gastric cancer cells from undergoing apoptosis. BMC Cancer. 2011;11:183.
11.　Chen J, Wang T, Xu S, et al. Discovery of novel antitumor nitric oxide-donating β-elemene hybrids through inhibiting the PI3K/Akt pathway. Eur J Med Chem. 2017;135:414.

12. Sun Y, Liu G, Zhang Y, et al. Synthesis and in vitro anti-proliferative activity of β-elemene monosubstituted derivatives in HeLa cells mediated through arrest of cell cycle at the G1 phase. Bioorg Med Chem. 2009;17:1118.

13. Wang B, Peng X, Sun R, et al. Systematic review of β-Elemene injection as adjunctive treatment for lung cancer. Chin J Integr Med. 2012;18:813.

14. Hu Q, Bai L, Zhu Z, et al. β-Elemene-loaded polymeric micelles intensify anti-carcinoma efficacy and alleviate side effects. Chinese Chem Lett. 2020;31:915.

15. Jiang L, Li A, Tan Y, et al. Clinical observation of elemene injection combined with cisplatin in the treatment of malignant pleural and peritoneal effusion. Med Sci J Central South China. 2020;48:428.

16. Wang Z, Li Y, Zhou F, et al. β-Elemene enhances anticancer bone neoplasms efficacy of paclitaxel through regulation of GPR124 in bone neoplasms cells. Oncol Lett. 2018;16(2):2143.

17. Cheng H, Ge X, Zhuo S, et al. β-Elemene synergizes with gefitinib to inhibit stem-like phenotypes and progression of lung cancer via down-regulating EZH2. Front Pharmacol. 2018;9:1413.

18. Gao Y, Mao N-D, Che H, et al. Novel hydroxyl carboximates derived from β-elemene: design, synthesis and anti-tumour activities evaluation. J Enzym Inhib Med Chem. 2022;37:2403.

19. Ye Y, Qi X, Xu B, et al. Nickel-catalyzed cross-electrophile allylation of vinyl bromides and the modification of anti-tumour natural medicine β-elemene. Chem Sci. 2022;13:6959.

20. Bai R, Zhu J, Bai Z, et al. Second generation β-elemene nitric oxide derivatives with reasonable linkers: potential hybrids against malignant brain glioma. J Enzym Inhib Med Chem. 2022;37:379.

21. Qi X, Jiang S, Hui Z, et al. Design, synthesis and antitumor efficacy evaluation of a series of novel β-elemene-based macrocycles. Bioorgan Med Chem. 2022;74:117049.

22. Kumar V, Kundu S, Singh A, et al. Understanding the role of histone deacetylase and their inhibitors in neurodegenerative disorders: current targets and future perspective. Curr Neuropharmacol. 2022;20:158.

23. He X, Li Z, Zhuo X-T, et al. Novel selective histone deacetylase 6 (HDAC6) inhibitors: a patent review (2016-2019). Recent Pat anti-Cancer Drug Dis. 2020;15:32.

24. Gao Y, Zhang H, Lirussi F, et al. Dual inhibitors of histone deacetylases and other cancer-related targets: a pharmacological perspective. Biochem Pharmacol. 2020;182:114224.

25. Newbold A, Falkenberg KJ, Prince HM, Johnstone RW. How do tumor cells respond to HDAC inhibition? FEBS J. 2016;283(22):4032–4046.

26. Marks PA, Rifkind RA, Richon VM, et al. Histone deacetylases and cancer: causes and therapies. Nat Rev Cancer. 2001;1:194.

27. Johnstone RW. Histone-deacetylase inhibitors: novel drugs for the treatment of cancer. Nat Rev Drug Discov. 2002;1:287.

28. Minucci S, Pelicci PG. Histone deacetylase inhibitors and the promise of epigenetic (and more) treatments for cancer. Nat Rev Cancer. 2006;6:38.

29. Barneda-Zahonero B, Parra M. Histone deacetylases and cancer. Mol Oncol. 2012;6:579.

30. Xu WS, Parmigiani RB, Marks PA. Histone deacetylase inhibitors: molecular mechanisms of action. Oncogene. 2007;26:5541.

31. Li Y, Seto E. HDACs and HDAC inhibitors in cancer development and therapy. Cold Spring Harb Perspect Med. 2016;6:a026831.

32. Bolden JE, Peart MJ, Johnstone RW. Anticancer activities of histone deacetylase inhibitors. Nat Rev Drug Discov. 2006;5:769.

33. Eckschlager T, Plch J, Stiborova M, et al. Histone deacetylase inhibitors as anticancer drugs. Int J Mol Sci. 2017;18:1414.

34. Gryder BE, Sodji QH, Oyelere AK. Targeted cancer therapy: giving histone deacetylase inhibitors all they need to succeed. Future Med Chem. 2012;4:505.

35. Shah MH, Binkley P, Chan K, et al. Cardiotoxicity of histone deacetylase inhibitor depsipeptide in patients with metastatic neuroendocrine tumors. Clin Cancer Res. 2006;12:3997.

36. Suraweera A, O'byrne KJ, Richard DJ. Combination therapy with histone deacetylase inhibitors (HDACi) for the treatment of cancer: achieving the full therapeutic potential of HDACi. Front Oncol. 2018;8:92.

37. Diyabalanage HV, Granda ML, Hooker JM. Combination therapy: histone deacetylase inhibitors and platinum-based chemotherapeutics for cancer. Cancer Lett. 2013;329(1):1–8.

38. Thurn KT, Thomas S, Moore A, et al. Rational therapeutic combinations with histone deacetylase inhibitors for the treatment of cancer. Future Oncol. 2011;7:263.

39. Luan Y, Li J, Bernatchez JA, et al. Kinase and histone deacetylase hybrid inhibitors for cancer therapy. J Med Chem. 2019;62:3171.

40. Li Y, Luo X, Guo Q, et al. Discovery of N1-(4-((7-Cyclopentyl-6-(dimethylcarbamoyl) -7H-pyrrolo[2,3-d]pyrimidin-2-yl)amino)phenyl)-N8-hydroxyoctanediamide as a novel inhibitor targeting cyclin-dependent kinase 4/9 (CDK4/9) and histone deacetlyase1 (HDAC1) against malignant cancer. J Med Chem. 2018;61:3166.

41. Huang Y, Dong G, Li H, et al. Discovery of janus kinase 2 (JAK2) and histone deacetylase (HDAC) dual inhibitors as a novel strategy for the combinational treatment of leukemia and invasive fungal infections. J Med Chem. 2018;61:6056.

42. Zhang K, Lai F, Lin S, et al. Design, synthesis, and biological evaluation of 4-methyl quinazoline derivatives as anticancer agents simultaneously targeting phosphoinositide 3-kinases and histone deacetylases. J Med Chem. 2019;62:6992.

43. Rangasamy L, Ortín I, Zapico JM, et al. New dual CK2/HDAC1 inhibitors with nanomolar inhibitory activity against both enzymes. ACS Med Chem Lett. 2020;11:713.

44. Liu J, Qian C, Zhu Y, et al. Design, synthesis and evaluate of novel dual FGFR1 and HDAC inhibitors bearing an indazole scaffold. Bioorgan Med Chem. 2018;26:747.

45. Zang J, Liang X, Huang Y, et al. Discovery of novel pazopanib-based HDAC and VEGFR dual inhibitors targeting cancer epigenetics and angiogenesis simultaneously. J Med Chem. 2018;61:5304.

46. He X, Zhuo X-T, Gao Y, et al. β-Elemene derivatives produced from SeO_2-mediated oxidation reaction. Royal Soc Open Sci. 2020;7:200038.

47. Watson PJ, Millard CJ, Riley AM, et al. Insights into the activation mechanism of class I HDAC complexes by inositol phosphates. Nat Commun. 2016;7:11262.

48. Miyake Y, Keusch JJ, Wang L, et al. Structural insights into HDAC6 tubulin deacetylation and its selective inhibition. Nat Chem Biol. 2016;12:748.